UNLV Theses, Dissertations, Professional Papers, and Capstones

2009

Soil moisture and water stage estimation using precipitation radar

Sumit Puri
University of Nevada, Las Vegas, er.sumitpuri@gmail.com

Follow this and additional works at: https://digitalscholarship.unlv.edu/thesesdissertations

Part of the Civil and Environmental Engineering Commons, Environmental Monitoring Commons, Fresh Water Studies Commons, and the Soil Science Commons

SOIL MOISTURE AND WATER STAGE ESTIMATION USING

PRECIPITATION RADAR

by

Sumit Puri

Bachelor of Engineering
Punjab Engineering College
Chandigarh, India
2006

A thesis submitted in partial fulfillment of
the requirements of the

Master of Science Degree in Civil Engineering
Department of Civil and Environmental Engineering
Howard R. Hughes College of Engineering

Graduate College
University of Nevada, Las Vegas
December 2009

THE GRADUATE COLLEGE

We recommend that the thesis prepared under our supervision by

Sumit Puri

entitled

Soil Moisture and Water Stage Estimation Using Precipitation Radar

be accepted in partial fulfillment of the requirements for the degree of

Master of Science
Civil Engineering

Sajjad Ahmad, Committee Chair

Thomas Piechota, Committee Member

Kumud Acharya, Committee Member

Ashok Singh, Graduate Faculty Representative

Ronald Smith, Ph. D., Vice President for Research and Graduate Studies
and Dean of the Graduate College

December 2009

ABSTRACT

**Soil Moisture and Water Stage Estimation
Using Precipitation Radar**

By

Sumit Puri

Dr. Sajjad Ahmad, Examination Committee Chair
Assistant Professor
University of Nevada, Las Vegas

In south-western United States, soil moisture data is important for drought studies
in the region which is experiencing a drought for many years, whereas in South Florida,
water stage data is required by hydrologists to monitor the hydrological flow in wetlands.
Soil moisture data and water stage data are not sufficiently available due to sparse
monitoring stations. Installation of dense measuring stations over an extended area is
costly and labor intensive. Therefore, there is a need to develop an alternative method of
measuring soil moisture and water stage.

Microwave remote sensing has proven to be a useful tool in the measurement of
various surface variables from space. This research explores the capability of microwave
remote sensing to measure soil moisture and water stage on the earth from space.
Tropical Rainfall Measuring Mission Precipitation Radar (TRMMPR) provides the *Ku*-
band backscatter measurements that are used to measure soil moisture and water stage.
Models that relate soil moisture and water stage to TRMMPR backscatter ($\sigma°$) are
developed. The dependence of $\sigma°$ on the dielectrical and physical characteristics of the

land surface is used as the basis of this research. The soil moisture content affects σ° by changing the dielectric constant of the surface whereas the vegetation density affects σ° by changing the physical characteristics of the surface. Vegetation density in the model is represented by Normalized Difference Vegetation Index (NDVI). Dependence of σ° on partial submergence of vegetation in inundated areas is used to measure water stage in wetlands of South Florida. The effects of the exposed vegetation above the water surface on the model are assessed by comparing two cases of model run– (a) that includes NDVI in the model, and (b) that does not include NDVI in the model.

Eleven years of data is used in this research where 75% of the data is used for calibration of the model and 25% of the data is used for validation. The estimated values of soil moisture and water stage are compared to the observed values and the performance of the models is assessed by calculating correlation coefficients, calculating root mean square errors, and plotting non-exceedance probability plots for the absolute error between observed and modeled values.

The soil moisture and water stage models work reasonably well and are able to estimate soil moisture and water stage with low errors. The soil moisture model works better in low vegetated areas because low vegetation allows the incident radiation to penetrate through the canopy cover and provide measurements from underlying surfaces. The water stage model works better in shrublands where there are no tree trunks and the model has an immediate impact from the vegetation canopy. This research provides an alternate way of measurement of soil moisture and water stage using remote sensing.

TABLE OF CONTENTS

LIST OF FIGURES

LIST OF TABLES

x

ACKNOWLEDGEMENTS

CHAPTER 1

INTRODUCTION

The southern regions of United States (US) are host to various water related problems. Long term droughts and floods are common in various parts of Southern US. Droughts severely damage the agricultural crops and impact the economic conditions of the affected area. Decrease in water levels in storage lakes and reservoirs can result in scarcity of water throughout the region. Such scarcity of water has a negative effect on the inhabitants, flora, and fauna of drought-affected regions. Due to the adverse effects of drought on socio-economic conditions it is imperative to study the factors influencing drought occurrence and severity. One of the factors that has the potential of predicting drought conditions is the spatio-temporal variation of water contained in the soil. The amount of recent precipitation, agricultural potential, and water storage is reflected in the soil water content and serves as an indicator of drought (Su et al., 2003). Thus, water present in the soil can provide insight into the drought conditions.

Parts of the southern US are also inundated perennially and constitute vast swamps and wetlands. These wetlands are habitat to diverse vegetation and wildlife. Wetland ecosystems have deteriorated in recent years due to various anthropogenic activities such as urban sprawl. Recently, efforts have been made by scientists and engineers to restore degraded wetland ecosystems. This requires understanding of the hydrological patterns of water flow in the area. Information on patterns of water stage can play a key role in the mitigation of anthropogenic impacts and help in the restoration

1

of the wetland ecosystem.

The water related problems in the southern US can be addressed by understanding the hydrological processes in the region. The understanding of these hydrological processes is important as it provides groundwork for future scientific studies.

Soil moisture measurements can help hydrologists, scientists, resource managers, and planners to effectively monitor drought conditions. Measurements of water stage are useful in restoring the fragile ecosystem of wetlands. High resolution maps could provide a comprehensive spatio-temporal behavior of soil moisture and water stage. However, soil moisture measurements are not available over large extended areas because their measurement stations are sparsely located. Even water stage measurements are not available because of limited number of water stage measuring stations. Installation of dense network of stations would involve high costs due to purchase of sophisticated instruments and hiring skilled labor to use those instruments. An alternate way to acquire soil moisture and water stage data is by employing space borne remote sensing.

Remote sensing in microwave portion of the electromagnetic spectrum is very advantageous for mapping land surface characteristics such as soil moisture and water stage. Microwave remote sensing is independent of solar illumination and provides day and night observations. It is less affected by the atmosphere and can provide observations in all weather conditions. Microwave remote sensing is also sensitive to dielectric properties of the surface and hence can be used to detect water. Microwave remote sensing is also sensitive to physical and geometrical characteristics of the land surface

2

and thus can be used to measure water stage.

The Tropical Rainfall Measuring Mission (TRMM) satellite was launched by NASA in December 1997 to study the rainfall patterns in tropical regions of the globe. Precipitation Radar aboard TRMM is a radar that operates in the *Ku*-band of the microwave region. It transmits a pulse of energy to the ground which scatters off the ground surface depending on its physical and electrical properties. The portion of energy scattered back to the radar receiver is referred to as backscatter. This backscatter can be used to understand the spatio-temporal extent of soil moisture and water stage.

1.1. Research Motivation

The southern US is experiencing different water resources issues in two different regions– western region and eastern region. Western parts of Southern US within the Colorado River Basin have endured drought like conditions since 2000. This has become the longest and worst drought in the past 80 years (Piechota et al., 2004). On the other hand, in south-eastern parts of US comprising of Everglades, serious efforts are being undertaken to restore the wetland ecosystem and mitigate the human activities for water supply, agricultural development, and flood control purposes that have disrupted the natural flow of water.

The Everglades are subtropical wetlands in Southern Florida which provide a unique habitat for a range of plant and animal species. This ecosystem has degraded and been reduced in size due to anthropogenic activities (Wdowinski et al., 2004). Recently,

3

efforts have been made to restore this habitat. Restoration efforts include restoring the natural hydroperiod that refers to the cyclic rise and fall of water levels corresponding to the seasonal variation in rainfall. Restoration of Everglades's hydroperiod is obstructed by dense network of manmade levees, flood gates and other control channels. This region has both a managed and natural flow wetland environment. Understanding the hydrological movements in wetlands requires the knowledge of water stage to assess the flow patterns.

Soil moisture and water stage measurement over large extent are required to understand drought conditions and restoring the wetland ecosystem, respectively. However, soil moisture and water stage data is scarce because existing observation sites are rare and sparse. *In-situ* measurement of these variables in the field is difficult and expensive. There is a need of alternate methods to measure soil moisture and water stage. Space-borne microwave remote sensing can be used to obtain a comprehensive spatio-temporal understanding of soil moisture and water stage.

Tropical Rainfall Measuring Mission Precipitation Radar (TRMMPR) has been providing land surface backscatter measurements since 1998. These backscatter measurements are sensitive to dielectric and physical properties of the land surface. The sensitivity to dielectric measurements can be linked to the moisture content in the soil. Physical properties of inundated areas affect backscatter measurements that can be linked to water stage. Availability of eleven years of TRMMPR data provides an opportunity to perform a long-term analysis of backscatter in relation to soil moisture

www.manaraa.com

and water stage.

1.2. Research Objectives

This research aims to develop models that can estimate the soil moisture and water stage from TRMMPR backscatter measurements. The soil moisture and water stage is related to backscatter measurements and dependence on the type and greenness of vegetation cover is investigated. The vegetation in the models is represented by the Normalized Difference Vegetation Index (NDVI), a measure of greenness of vegetation. Both the soil moisture model and water stage model are point based empirical models that are assumed to be linearly related to backscatter and NDVI. The models are calibrated using the ground measurements of soil moisture and water stage over several ground stations in various landcovers. The calibrated models are then used to estimate soil moisture and water stage at the measuring sites. Modeled soil moisture and water stage is compared with ground measurement to assess the accuracy of the model.

Key research questions addressed in this study are as follows.

1. Can active sensors such as TRMMPR be used to measure soil moisture?

2. How is TRMMPR backscatter measurements related to water stage?

3. What is the affect of vegetation on the relationship of backscatter and soil moisture?

4. How does vegetation impact the relationship between backscatter and water stage?

In order to address the above mentioned research questions, following tasks are undertaken.

1. Orbital TRMMPR backscatter data from NASA, soil moisture data from Soil Climate Analaysis Network, water stage from South Florida Water Management District, landcover classification map from University of Maryland, and NDVI from Advanced Very High Resolution Radiometer are obtained.

2. The soil moisture, water stage, and NDVI data is averaged to match with the temporal resolution of backscatter data used in both the models.

3. A model relating soil moisture with backscatter and NDVI is developed.

4. A model that relates water stage to backscatter is developed. The effect of NDVI on the model is also assessed.

5. The soil moisture model is calibrated and validated using ground measurements of soil moisture over Southern United States.

6. Water stage model is calibrated and validated in South Florida.

7. The modeled values of soil moisture and water stage and their observed values are compared and the accuracy of the models at various sites is assessed.

This research is organized as follows. Chapter 2 presents a review of literature that describes the study areas, and existing methods used to measure soil moisture and water stage. The advantages of microwave remote sensing and characteristics of TRMMPR backscatter are also presented. Furthermore, the effects of vegetation on the backscatter used to measure soil moisture and water stage are discussed. Chapter 3 is a manuscript titled, 'Relating Surface Backscatter Response from TRMMPR to SCAN Soil Moisture in Southern United States'. This manuscript describes the soil moisture

www.manaraa.com

model and the model parameters. The water stage model is described in Chapter 4 which consists of the manuscript titled, 'Estimation of Water Stage over wetlands of South Florida using TRMMPR observations'. Finally, the conclusions and recommendations are presented in Chapter 5.

CHAPTER 2

LITERATURE REVIEW

This chapter is organized as follows. Section 2.1 discusses the study area, its historic growth and climatic conditions. The physical features of Southern United States and South Florida that contribute to drought and wetland ecosystem, respectively is also discussed in this section. Section 2.2 describes the importance of soil moisture and water stage in the study area. Different techniques used to measure soil moisture and water stage are also described. Section 2.3 describes the characteristics of TRMMPR backscatter and its role in determination of soil moisture and water stage. The effects on vegetation are also summarized in the form of NDVI that serves as an index of vegetation.

2.1.   Study Area

There are two areas of study in this research. The soil moisture mapping is done in southern US and water stage modeling is carried out in South Florida. The characteristics of each of the study area are described below.

2.2.   Southern United States

The Southern US studied in this research comprises of Arizona and New Mexico in the west, Texas and Oklahoma in the mid-west, and Mississippi, Alabama, Georgia, South Carolina, and Florida in the east. Figure 1 shows the map of US. The Southern

US has a varied topography. A broad, flat coastal plains spreads from Texas to Florida peninsula. The southeastern part of US mainly consists of sub-tropical forests. Mangrove wetlands cover a majority part of Florida. The Appalachian Mountains lie in the northern parts of Alabama and Georgia. West of the Appalachian Mountains, is the Mississippi river basin. The mid-west region near the basin mainly consists of rolling hills and productive farmlands. The Great Plains lie west of Mississippi river basin and east of Rocky Mountains. Majority of the agricultural produce is grown in the farmlands of these Great Plains. The low relief of the area suddenly changes to mountain ranges in the Rocky Mountains. Rocky Mountains extend from Canada in the north to Mexico in the south. Rocky Mountains in the southern US consists of various smaller mountain ranges forming a large number of valleys and basins. The south western areas mainly comprise of desert and arid regions. These areas receive rainfall of less than 0.5 ft in an year whereas eastern coast receives rainfall on the order of 5 ft/year.
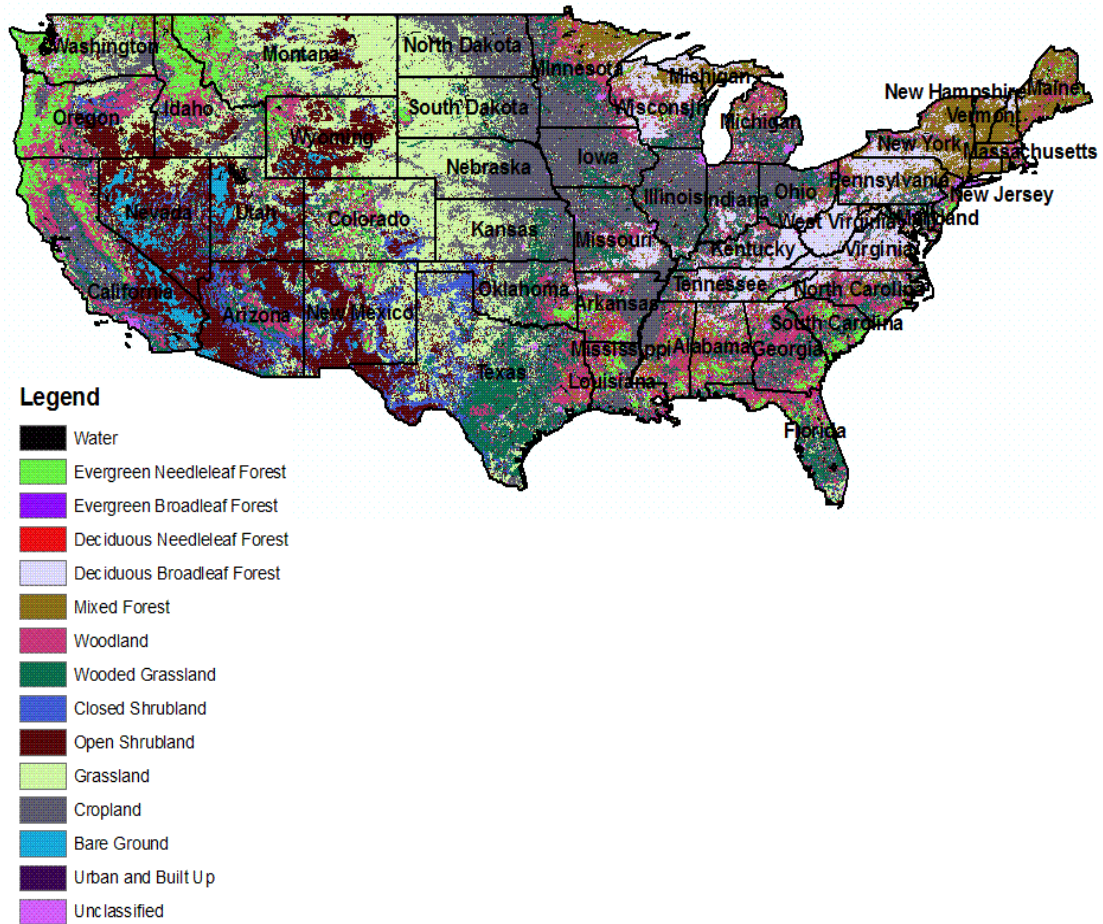
Figure 1 Landcover Map of United States.

The varied topography from mountains in the south-west to plains in the mid-west and wetlands in the south-east, is subjected to varied types of landuse and landcover. The arid and semi-arid western ranges that is mostly covered by deserts is home to open shrublands and bare ground. In open shrublands canopy cover lies between 10% to 40%. The remaining cover is mostly barren. The tree heights in open shrublands are less than 6 ft (Hansen et al., 2000). This land type is mostly due to the lack of rainfall in the region and its arid climate. There is a transition from open shrublands to grasslands moving towards the Great Plains.

10

This area covered by Great Plains consists of grasslands and wooded grasslands. Grasslands consist of herbaceous cover with very few trees or canopy cover. The wooded grasslands have less than 40% cover of trees where tree heights are less than 15 ft. This area also contains closed shrublands which differs from open shrublands in terms of tree height and canopy cover of bushes and shrubs. The tree height in closed shrubland is not more than 15 ft whereas in open shrublands tree heights do not increase more than 6 ft. The percent canopy cover of bush and shrub is less than 10% in open shrublands. On the other hand, bush and shrub canopy cover in closed shrubland lies between 10% and 40%.

The Mississippi river basin and the area east to it mainly comprises of woodlands and croplands though little presence of evergreen forests is also observed. Tree heights in the woodlands exceed 15 ft and the tree canopy cover is between 40% and 60%. Croplands on the other hand consist of crop producing fields that span more than 80% of the cover. The patches of evergreen forests remain green throughout the year with tree heights exceeding 15 ft. These forests are abundant with trees with their canopy exceeding 60% of the area. The south-eastern parts of US are abundant with wooded grasslands and grasslands that form the mangrove wetlands. The major landcover types of Southern US are summarized in Table 1.

11

Table 1 Summary of various landuse types in Southern US (Hansen et al., 2000).

Landuse Type	Tree Height	Canopy Cover	Dominant areas
Bare Ground	-	< 10% vegetation	South-western
Open Shrublands	< 6 ft	10% < bush/shrub < 40%	South-western
Closed Shrublands	< 15 ft	Bush/shrub > 40%	Mid-west
Grasslands	-	Herbaceous cover	Mid-west
Wooded Grasslands	> 15 ft	10% < tree canopy < 40%	Mid-west
Woodlands	> 15 ft	40% < tree canopy < 60%	South-eastern
Croplands	-	Crop producing fields	South-eastern
Forests	> 15 ft	Tree canopy > 60%	Eastern

2.3. South Florida

South Florida is geographically defined by water as it is surrounded by Atlantic Ocean on one side and Gulf of Mexico on the other two sides. It consists of thousands of small lakes and water bodies. The largest lake in the region is Lake Okeechobee that occupies 730 square miles of the area. It is a shallow lake with mean depth of 9 ft. Generally lake levels are maintained between 13 ft to 15 ft of National Geodetic Vertical Datum (NGVD) that makes the storage capacity to 300, 000 ac-ft. Lake Okeechobee has many waterfowl (ducks, swans, etc.) as breeding and brood-rearing habitat. The littoral zone of the lake that spans about 150 square miles is home for nesting fish and wading birds.

Kissimmee River lies to the north of the lake and drains into Lake Okeechobee. Caloosahatchee River on the western side and St. Lucie Canal on the eastern side are two outlets of the lake that drains into Gulf of Mexico and Atlantic Ocean, respectively. The Everglades Agricultural Area (EAA) lies to the immediate south of the Lake Okeechobee. Many canals run through the EAA originating from the Lake Okeechobee

to the Atlantic Ocean as shown in Figure 2. Adjacent to EAA are the Water Conservation Areas (WCAs) that store the surplus water in the region. This region has the maximum number of manmade levees and water control structures. There is a complex interaction between manmade and natural features in this region. The Lower East Coast (LEC) comprises of various urban cities such as Miami, West Palm Beach, and Fort Lauderdale. This densely populated area lies near the lower south eastern coast adjacent to low-lying Everglades National Park (ENP) and agricultural land on the west. ENP is covered mainly with the tropical and sub-tropical forests and preserves the natural environment of Everglades.

The South Florida region is characterized by heavy rainfall of about 3.6-4.5 ft/yr that results in large volumes of surface water. Most of this water evaporates, infiltrates or drains to the ocean. One of the major economic activities of the region is agriculture that is abundant in the interior of South Florida. The climate of South Florida is favorable to growth of large variety of crops throughout the year. Sugarcane and citrus fruits are the major agricultural produce of the region. These large scale agricultural practices in South Florida started in 1920 after draining large volumes of peat soil from the region. This increased the agricultural water demand in the region. This water demand was further increased with growing human population in the surrounding areas of LEC.

Human settlements on the Atlantic Coastal Ridge started because the location was favorable for marine trade. The urbanization led to increase in development of

agricultural areas and flood control structures which ultimately led to draining of Everglades. South Florida faces a common problem of saltwater intrusion. The region consists of various canals that drain from interiors of South Florida and drains to nearby Gulf of Mexico or Atlantic Ocean. These canals lower the water table and allow the intrusion of seawater. During dry season and periods of droughts, the seawater moves inland through the canals and infiltrates into the aquifers. Lowering of ground water table creates a negative head and allows the seepage of saltwater into the aquifers. However, the problem of uncontrolled saltwater intrusion has been addressed by construction of various control structures near the outlets of the drainage canals. These controls are opened to release excess of water during rainy seasons to avoid flooding in the region. During the dry season, these gates are closed to prevent the intrusion of seawater through canals. South Florida Water Management District (SFWMD) is a government agency that operates the water control structures in South Florida to prevent flooding and regulate the water flow. In certain areas, mainly WCAs the operation of the flood control structures result in the accumulation of water in excess of natural background levels (Wdowinski et al., 2008).
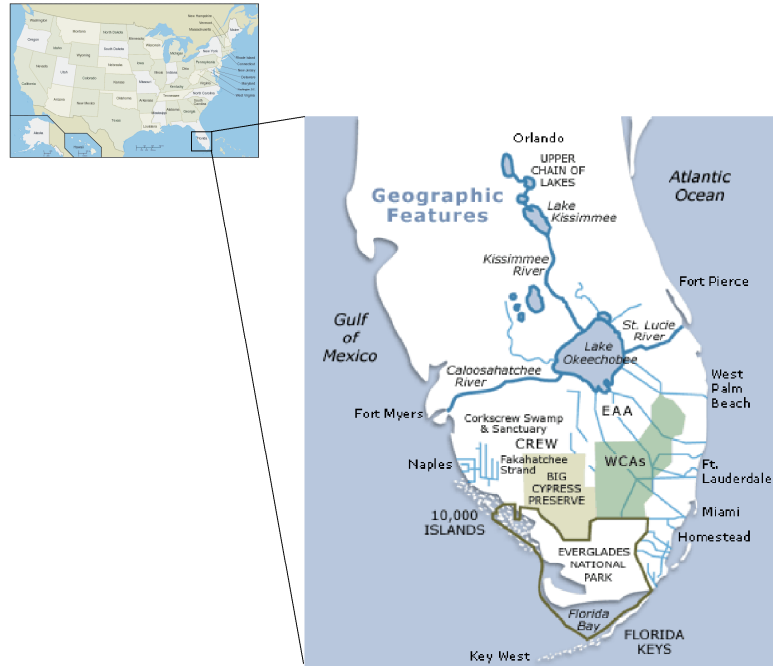
Figure 2 Geographical features of South Florida (Source: SFWMD website).

2.4. Ground Data

The measuring stations for soil moisture and water stage are sparsely located and hence measurement of soil moisture and water stage at a large spatial scale is not possible. This research proposes an alternate way of measurement of soil moisture and water stage that uses remote sensing techniques. In order to validate the method proposed in this research. The ground data of soil moisture and water stage at available stations is hence used. The importance of soil moisture and the reasons for which it should be monitored at large spatial scales is described below.

2.5. Soil Moisture

Soil moisture (m_s) is an important factor in global hydrological circulation and

15

plays a significant role in the research of hydrology, climatology, and meteorology (Schneider et al., 2008; Das et al., 2008; Song et al., 2007). m_s is an important variable in the hydrological cycle. It plays a critical role in various environmental processes because it is the only variable that influences the land surface interactions with the atmosphere by describing the water and energy exchanges. m_s plays a critical role in many hydrological processes including infiltration, evaporation, and runoff. Soil moisture regulates the surface thermodynamics and determines the distribution of incident solar radiations into sensible and latent heat thus, governing the evapotranspiration. On the basis of evapotranspiration, differential surface heating of the land takes place that results in convective behavior of atmospheric particles and winds. The differential surface heating influences water and energy exchanges at the interface of land with atmosphere through feedback between precipitation and soil moisture.

The feedback between precipitation and soil moisture is useful in understanding the hydrological relationship between rainfall and surface runoff. m_s influences the division of rainfall into infiltration and surface runoff. A saturated land mass rainfall generates more runoff as compared to dry land mass where majority of the water percolates into the ground and adds to the ground water table or becomes part of the base flow.

m_s status in the root zone is an important component of the water cycle at point, field, catchment, watershed, and regional scales. This makes monitoring soil moisture important for making irrigation scheduling decisions. Lower soil moisture content

16

results in improper nourishment of crops whereas; higher moisture content leads to leaching of nutrients vital for crops. Since soil moisture has the potential to affect both rainfall and irrigation, accurate knowledge of soil moisture can provide a good insight into drought conditions of an area.

Soil moisture is highly variable both spatially and temporally. In spite of being such an important variable, m_s data is not sufficiently available. Soil moisture measurements from the experiments are available at only few selected locations (Wagner et al., 2003; Das et al., 2008). Measuring m_s is a difficult task because it involves costly instruments and skilled labor. Description of some of the traditional methods used to measure m_s with their advantages and disadvantages are provided below.

Gravimetry

Gravimetry is based on the traditional method of sampling and drying. The soil samples are collected at desired locations and depth using augers and drills. These soil samples are then taken to a laboratory and weighed. The samples are then oven dried for 24 hours and dried weight is measured again giving the volume of water present by weight in the sample. This method is simple and easy to use. It is also less costly as it does not need any sophisticated instruments. Gravimetric soil moisture can be converted to volumetric soil moisture using conversion formulas. The disadvantage of this method is it takes a long time for the oven drying process. Also the process of obtaining the soil samples using augers and drills disturbs the natural setting of the soil mass.

17

Tensiometry

This technique is widely used by farmers to assess the need for irrigation of crops. Tensiometer is a simple instrument and is generally installed in pairs. One tensiometer is inserted in the ground at shallow depths to measure the moisture in the root zone of soil layer and the other at deeper location to monitor the moisture conditions below the soil root zone. The basic principle behind the instrument is to measure the tension by which water is entrapped in the soil. For a near saturated condition when sufficient water is stored in the soil, there is less tension in the soil to hold the water particles. However, as the water content gets depleted, the soil particles hold the water more tightly thereby increasing the tension. Tensiometers consist of a bulb of porous ceramic substance and needs to be installed very carefully. It gives a reading of zero for saturated soil and higher reading of around 85 for drier soil. Though a simple method, tensiometers need maintenance at a regular interval.

Time Domain Reflectometry (TDR)

Time Domain Reflectometer is an electrical instrument that measures the dielectric constant of a soil. It consists of a transmitter and a receiver. The transmitter sends a signal into the soil mass and the receiver receives the signal after a time lag. This time lag in a soil depends on the dielectric constant of the soil which is a measure of the moisture in the soil. Soils with high moisture content have a high dielectric constant that produces longer time lag between transmitted and received signals. This method of measurement of soil moisture is costly because of the expensive electrical

instrument involved.

<u>Neutron Probe (NP)</u>

The Neutron probe method is based on the flux of slowing neutrons. Presence of hydrogen in any substance decreases the motion of the neutrons. Soil contains hydrogen as organic matter or other material and in the form of the water. Quantity of hydrogen present in the form of organic and other matter is dependent on the soil texture and the type of soil and doesn't change over time. However, hydrogen present in water molecules, changes with the variation in the moisture content of the soil. This change in hydrogen is detected by slowing speeds of neutrons. The major disadvantage of this method is that it requires the calibration of the instrument repeatedly. Due to exposure to gamma radiations and neutrons, it poses a health hazard to users.

The soil moisture data is this research is obtained from Soil Climate Analysis Network (SCAN) that measures the ground m_s using Hydra probe II SM sensor and provides hourly values of volumetric m_s. The Hydra Probe is a Frequency Domain Reflectometer. It consists of capacitance plates inserted in the soil medium forming a capacitor. The capacitance changes with the change in dielectric constant of the soil medium. Hence, any changes in the soil moisture content are reflected in the capacitance of the capacitor. An oscillator is used in the setup to complete the circuit. With the change in capacitance induced by the soil moisture variation, the operating frequency of the circuit varies. This frequency variation is used to measure the soil moisture by the Hydra probe sensor.

A soil sample consists of solid soil particles and voids that are occupied by water and air as shown in Figure 3. In a relatively dry soil sample, the water molecules are tightly held by the soil particles. As the water content increases, water moves more freely in the soil mass. This free movement of water in the soil increases the dielectric constant of the soil. The dielectric constant (ε) of water is very high ($\varepsilon \sim 80$) as compared to dry soil mass which has very low dielectric constant ($\varepsilon \sim 6$). The microwave remote sensing techniques being sensitive to dielectric properties of surface use this difference in ε to measure soil moisture in a soil sample. The microwave remote sensing techniques to measure soil moisture are described in detail in the subsequent sections.
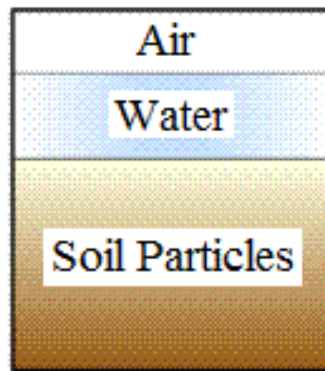
Figure 3 A sample of soil mass.

2.6. Water Stage

Areas like wetlands and swamps are inundated with water throughout the year. They form a distinct ecosystem with diverse flora and fauna. Wetlands provide habitat for waterfowl, fish, and wildlife. It supports rich biodiversity including threatened and

endangered species (Ozesmi and Bauer, 2002). Wetland inundation assists in ground water recharge (Daily et al., 1997) and improves the water quality. Flooding and changes in water levels in wetlands play an important role in regulating the flow of water in these areas. Flooding impacts the hydrology, ecology, biology, and geochemistry of the lakes and wetlands (Zhang, 2008). Fluctuations in water stages in wetlands impact the nesting patterns of waterfowl by affecting their food supply (Swanson, 1988; Swanson and Duebbert, 1989; Covich et al., 1997). It changes the water salinity thereby modifying the vegetation patterns of wetlands (Gorham et al., 1983; LaBaugh et al. 1996; Mulhouse and Galatowitsch, 2003; van der Valk, 2005). In addition to this, different water stages are associated with different flow paths between surface water and ground water (Johnson et al., 2004).

After the beginning of 20th century, various anthropogenic impacts due to residential water demand, agricultural water demand and flood control purposes degraded the natural flow of wetland environment and adversely affected the ecology in the area. The agricultural activities damage the wetlands because of the sediments and pollution from fertilizers and pesticides (Martin and Hartman, 1987). Recently many efforts have been made to restore the wetland ecosystem. This requires understanding the hydrology of the area. Since these wetlands comprise of several lakes and water bodies of various sizes, tremendous hydrological variability of annual and inter-annual time scales is exhibited (Zhang, 2008). Due to geological complexity and lack of hydrological surveys, the smaller bodies of water are not monitored significantly which

21

makes the estimation of water stage on ground difficult to measure.

Determination of water stage changes is important for hydrological modeling and understanding of wetland ecosystem (Bourgeau-Chavez et al., 2005). However, the in-situ stage measurements are not available at an extensive network which has led to research on the use of microwave remote sensing in monitoring water stage (Alsdorf et al., 2000). Several studies have been carried out to monitor water stage using imaging radar such as Synthetic Aperture Radar (Kasischke et al., 2003; Wdowinski et al., 2004; Hess et al., 1995; Wang et al., 1995), passive microwave sensors (Sippe et al., 1998), and landsat thematic mapper (Mertes et al., 1995). The concept of remote sensing of water stage is based on the double-bounce reflection of the transmitted radar signal that takes place from the horizontal water surface and vertical vegetation (Richards et al., 1987). In non-vegetated areas, the water surface acts as a mirror and specular reflection of the transmitted radar signal takes place from the surface of the water.

Detection of water stage depends on the wavelength of imaging radar. Long wavelength, such as L-band (23 cm) can detect water stage changes beneath dense vegetation canopies as the incident radiations are able to penetrate through the canopy (Hess et al., 1990; Pope et al., 1994). Relatively shorter wavelength such as C-band (5.6 cm) can effectively monitor water level changes of herbaceous wetland ecosystem (Bourgeau-Chavez et al., 2005). In this research, the incident radiations from Ku-band (2.2 cm) are investigated over Everglades in South Florida and the dependence of backscatter on the partial submergence of vegetation in water is explored.

22

The stage data for this research is obtained from South Florida Water Management District (SFWMD) database. The stage data is provided as daily average levels above the National Geodetic Vertical Datum of 1929 (NGVD29). SFWMD monitors a network of control stations that provide daily average estimates of water level, rainfall, and other key hydrologic parameters. Most of the stage measurement stations are located near the water control structures for logistical and operational reasons (Wdowinski et al., 2008). As a result, interiors of natural flow wetlands are sparsely monitored. Hence, efforts have been in the field of space based remote sensing that provides high spatial resolution measurements of water level over wide areas.

2.7.   Microwave Remote Sensing

Remote sensing in the microwave region of the electromagnetic spectrum is called Microwave Remote sensing. The electromagnetic spectrum with the frequency range of microwave band is shown in Figure 4.
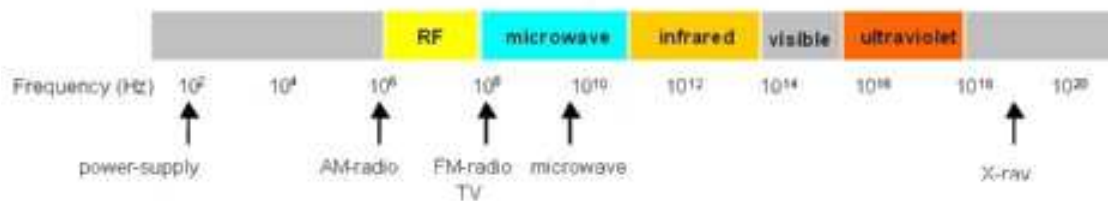
Figure 4 Electromagnetic Spectrum.

Microwave remote sensing is carried out in the microwave region of the

electromagnetic spectrum with frequency ranging from 0.3 GHz to 300 GHz (wavelength range from 0.1cm to 100cm). Microwave remote sensing is sensitive to physical and electrical properties of the land surface and thus can be used to monitor the surface characteristics. The major advantages of microwave remote sensing are (a) It does not depend on sun for source of illumination, and (b) It easily passes through vegetation and clouds and is not interfered by atmospheric effects (Njoku and Entekhabi, 1996). Both active and passive form of remote sensing has been used in the past to capture the surface characteristics of the land. Active microwave remote sensing is characterized by having its own source of illumination; passive microwave remote sensing uses sun as it source of energy.

Microwave remote sensing is sensitive to the dielectric properties of volumetric soil moisture (Ulaby et al., 1986). It is also sensitive to the texture of soil and can distinguish between different types of soil- sand, silt and clay at frequencies less than 10GHz if the soil is dry. At greater frequencies, it is difficult to differentiate between different types of soils. Both active and passive microwave remote sensing techniques have shown their potential for measurements of soil moisture (Wagner et al., 2003; Verhoest et al., 1998; Gao et al., 2006; Engman and Chauhan, 1995). Not even microwaves, but optical remote sensing and Global Positioning System (GPS) have also been used to map soil moisture in the past (Larson et al., 2008). The passive sensors (radiometers) detect the naturally emitted microwave radiations from the ground surface. However, in order to obtain the signal, sufficient amount of energy should be

24

detected by the radiometer. This results in high fields of view that makes spatial resolution very low (generally greater than 1 km) (Barrett et al., 2009). Many studies have been carried out to measure soil moisture using passive sensor (Jackson, 1993; Wigneron et al., 1998; Du et al., 2000; Li et al., 2002).

Although a lot of progress has been made with passive microwave sensors to monitor soil moisture (Moran et al., 2006), active sensors provide a higher spatial resolution for mapping soil moisture over a large coverage area. Active microwave sensors provide their own illumination and capture the signal on the basis of difference between transmitted and received microwave radiations. Thus, active sensors do not depend on the amount of energy emitted from land surface naturally and this results in higher spatial resolution. Mapping of soil moisture using active sensors is described in numerous studies (Ulaby and Batlivala, 1976; Ulaby et al., 1978; Jackson et al., 1981; Wang et al, 1986; Dobson and Ulaby, 1986; Oki et al., 2000). Active sensors can be divided into two categories: imaging (radar) and non-imaging sensors such as altimeters and scatterometers. Altimeters are used to measure heights over oceans and cryosphere; scatterometers are primarily used to measure wind speed and wind direction over ocean surfaces (Barrett et al., 2009).

Not only active and passive sensors but also many field experiments have been carried out to correlate spatial and temporal variability of soil moisture with remote sensing measurements. Some of the field experiments done are Washita' 92 (Jackson et al., 1995), Washita 1994 (Wang et al., 1997), SMEX02 (van Zyl et al., 2003), SMEX03

(Jackson et al., 2005), SMEX04 (Vivoni et al., 2008), and SMEX05 (Pauwels et al, 2008).

Microwave remote sensing can thus effectively provide soil moisture values at a large scale over a long period of time. It is a promising method for soil moisture estimation (Crosson et al., 2002; Paloscia et al., 2001). Hence, there has been a rising interest in remote sensing techniques with applications to the measurement of soil moisture (Wagner et al., 1999; Njoku et al., 2003; Moran et al., 2004). This research uses active microwave sensor Precipitation Radar to monitor soil moisture which is described in subsequent sections.

2.8. Tropical Rainfall Measuring Mission

Tropical Rainfall Measuring Mission (TRMM) is a joint mission between National Aeronautics Space Administration of USA and National Space Development Agency of Japan. It was launched on 27 November 1997 and data became available the next month in December (Kummerow et al., 2000). TRMM operates in a 350-km circular orbit with an inclination of 35°. The objectives of TRMM are to measure rainfall and energy exchange of tropical and sub-tropical regions of the world. The primary instruments aboard TRMM are Precipitation Radar (PR), TRMM Microwave Imager (TMI), Visible Infrared Scanner (VIRS), Lighting Imaging Sensor (LIS), and Clouds and Earth's radiant Energy System (CERES). A diagram of TRMM and the instruments aboard it are shown in Figure 5.

26
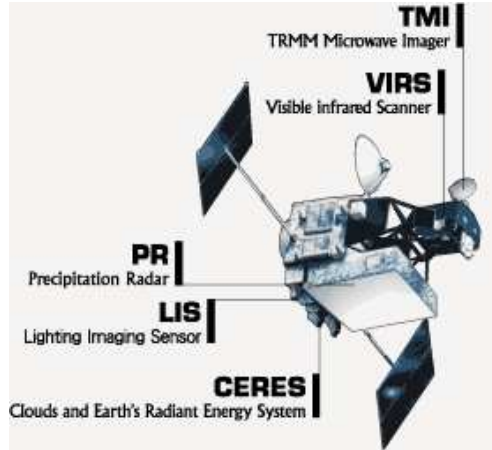
Figure 5 Instruments aboard TRMM (Source: NASA website).

2.9. TRMM Precipitation Radar

Precipitation Radar is an imaging radar sensor aboard the TRMM satellite which was developed by NASDA and Communications Research Laboratory, Ministry of Posts and Telecommunications. Precipitation Radar, operating at 13.8 GHz and 2.2 cm of wavelength has a sophisticated cross-track scanning over a swath width of 215 km with a cross-range spatial resolution of about 4.3 km. It has a vertical resolution of 250m (Kozu et al., 2001) that helps in profiling of three dimensional structure of rainfall.

Tropical Rainfall Measuring Mission Precipitation Radar (TRMMPR) backscatter ($\sigma°$) is the amount of energy scattered back to the receiver from the land surface. The intensity of $\sigma°$ is a function of physical and electrical properties of the target along with the wavelength, polarization and incidence angle of the incident energy. Since $\sigma°$ is a function of numerous variables, it is difficult to interpret the signals specifically from soil moisture or water stage. $\sigma°$ depends on surface

27

characteristics of the area including: landuse, landcover, type of soil, vegetation density, surface roughness, and moisture content of vegetation and soil. It is difficult to separate the effects of vegetation and surface roughness from the dielectric properties. The vegetation canopy absorbs and scatters most of the microwave radiation incident on it. The amount of energy absorbed is because of the canopy moisture content whereas the scattering is a result of the geometrical characteristics of its leaves. The effect of vegetation decreases as the wavelength increases (Ulaby et al., 1981). Shorter wavelengths such as X-band (λ=3 cm) reflect from the upper surface of canopy whereas longer wavelength such as L-band (λ= 24 cm) penetrate through the vegetation canopy and reflect from soil surface. All the intermediate wavelength bands reflect from both vegetation canopy as well as soil surface. For optimum soil moisture retrieval, it is recommended to use longer wavelength with low incidence angles so as to minimize the effects of vegetation and surface roughness. This research uses TRMMPR with λ= 2.2 cm. The study area in this research comprises of patchy vegetation that allows us to measure soil moisture effectively over the study area. Surface roughness is another variable that interferes in the mapping of soil moisture. It is statistically defined in terms of root mean square height, correlation length, and autocorrelation function. Determining surface roughness and separating its effects from vegetation is a challenging task. For incidence angles greater than 10°, the energy scattered back to the sensor increases with the increase in surface roughness (Ulaby and Batlivala, 1976). Hence, it is recommended to map surface characteristics such as soil moisture and water

28

stage at an incidence angle of 10°.

2.10.   NDVI

The Normalized Difference Vegetation Index is a simple numerical indicator used in remote sensing to assess the quantity of live green vegetation on the land surface. NDVI ranges from -1 to +1. Negative values of NDVI correspond to barren areas of rock, sand, or snow. Values close to zero from -0.1 to 0.1 generally correspond to water and low, positive values in the range of 0.2-0.4 indicate the presence of shrub and grassland, whereas high values approaching 1.0 represent temperate and tropical rainforests.

Live green vegetation absorbs solar energy most of which consists of radiation in the Near Infra Red (NIR) region for the purpose of photosynthesis. The leaf cells in the vegetation reflect and transmit the radiations in the Red Band of the electromagnetic spectrum. This is the basis of computation of NDVI based on the ratio of spectral reflectance in NIR and RED region. Mathematically, NDVI is calculated as shown in equation 2.1.

$$NDVI = \frac{NIR - RED}{NIR + RED} \qquad \text{Eqn. (2.1)}$$

where RED and NIR stand for the spectral reflectance measurements acquired in the red and near-infrared regions, respectively.

NDVI of an area consisting of dense vegetation canopy tends to take positive

values from around 0.3 to 0.8. Clouds and snow fields produce negative values of NDVI. Various water bodies like oceans, seas, lakes and rivers have a low reflectance in both NIR and RED bands. This results in low positive or slight negative NDVI values. Soils also generate small positive values of NDVI because of their larger NIR spectral reflectance than Red. NDVI values are affected by atmospheric effects. The atmospheric composition that includes water vapor and aerosols hamper the space borne NDVI measurement. Clouds also largely affect the NDVI data and leads to misrepresentations of a land surface.

2.11. Summary

Soil moisture and water stage data is of extreme importance to understand various hydrological processes. Sparsely located measurement stations do not provide soil moisture and water stage data over a large area for a long duration of time. Remote sensing is a useful tool that can be used to monitor soil moisture and water stage variation from space. Microwave remote sensing proves very advantageous in this regard. The backscatter measurements are sensitive to surface physical and electrical properties. Soil moisture is detected by TRMMPR backscatter in terms of dielectric constant of soil which is a measure of moisture contained in the soil. Water stage is detected by TRMMPR backscatter that measures the physical characteristics such as vegetation and surface roughness of the surface. The vegetation parameter is taken into account by using NDVI that serves as a measure of live green vegetation.

CHAPTER 3

RELATING SURFACE BACKSCATTER RESPONSE FROM TRMMPR TO SCAN

SOIL MOISTURE IN SOUTHERN UNITED STATES

3.1.   Abstract

Soil Moisture is an important variable in the hydrological cycle and plays a vital role in agronomy, meteorology, and hydrology. It regulates the exchange of water and heat between land surface and atmosphere and thus plays an important role in the development of weather patterns. It is difficult to obtain a comprehensive spatio-temporal map of soil moisture at river basin level because of the high costs of instrumentation.

In this paper, a model is developed that estimates soil moisture (ms) using backscatter from Tropical Rainfall Measuring Mission Precipitation Radar (TRMMPR) and Normalized Difference Vegetation Index (NDVI) over selected points in southern parts of United States. Soil moisture measured at 47 Soil and Climate Analysis Network (SCAN) stations is used to calibrate and validate the model. SCAN stations are spread across 970,000 square miles and are representative of various vegetation densities.

An empirical model that relates ms to TRMMPR backscatter ($\sigma°$) and NDVI is developed. The $\sigma°$ measurements are normalized at an incidence angle of 10°. Model is calibrated using 75% of the measured soil moisture data and validated using the remaining 25%. The estimated values of ms compare well with the ground

31

measurements. The model works well for various landcovers but works best for low vegetated areas. Closed shrubland are low vegetated areas characterized by low NDVI values (0.29-0.35). All the soil moisture estimates in this landcover have an absolute error of less than 8%. Overall, the model performance is satisfactory as it gives an absolute error of 10% or less for 90% of the estimates. Estimation of soil moisture at such a wide extent of area with a low magnitude of error provides an additional utility of TRMMPR data.

3.2.   Introduction

Soil moisture (m_s) is an important variable in the hydrological cycle (Bindlish et al., 2003; Schneider et al., 2008; Das and Mohanty, 2006; Song et al., 2007; Verhoest et al., 1998). It plays a critical role in many hydrological processes such as precipitation, runoff, percolation, infiltration, and evaporation. m_s plays a key role in splitting the rainfall into runoff and baseflow. The distribution of incident solar energy into the sensible and the latent heat depends on the moisture content of the soil (Houser et al., 1998). m_s can serve as an indicator of drought (Su et al., 2003) and thus accurate soil moisture information can provide insight into drought conditions.

Monitoring m_s is essential for an effective irrigation management in agriculture. m_s is a key component of irrigation scheduling decision used to prevent over irrigation that results in waste of water and fertilizers through leaching. It also helps keep a check on under irrigation that results in immature nourishment of crops.

32

m_s is highly variable spatially and temporally and its measuring stations are sparse (Wagner et al., 2003; Das et al., 2008). Remote sensing with its ability to cover larger area at finer spatial and temporal resolution provides an opportunity to measure soil moisture from space. Both active and passive remote sensing has been used for m_s measurement. Some of the approaches that use passive techniques of microwave remote sensing to measure soil moisture have been presented by Wigneron et al., 1998 and Jackson, 1993 in which the sensitivity of microwave remote sensing to dielectric properties of land surface is used to develop algorithms to map m_s over extended areas. Passive microwave sensors are less sensitive to the surface roughness and thus used for monitoring soil moisture at a global level (Oki et al., 2000). Passive microwave sensors detect the naturally emitted radiations from the land surface that results in low spatial resolution. On the other hand, active microwave sensors such as Tropical Rainfall Measuring Mission Precipitation Radar (TRMMPR) measure the difference in power between transmitted and received radiation that is affected by m_s. Albeit primarily designed to estimate vertical profile of rain, TRMMPR provides the surface backscatter measurements that can be related to the various characteristics of the land surface such as albedo, biomass, vegetation, and soil moisture.

In this paper, an empirical model is developed that relates m_s to TRMMPR backscatter ($\sigma°$) and Normalized Difference Vegetation Index (NDVI). $\sigma°$ depends upon dielectric constant, vegetation density and roughness of the surface. Since dielectric constant of wet soils is greater than that of dry soils, this difference is reflected in $\sigma°$

33

measurements and used to measure m_s. In the case of vegetated areas, the incident TRMMPR radiations are backscattered and reflected by the leaves in the vegetation canopy and are not able to provide the ground surface measurements. This effect of vegetation density and surface roughness is incorporated into the model by using NDVI. The model relates the volumetric m_s in percentage (%) to $\sigma°$, measured in decibels (dB) and NDVI (unitless). The model is calibrated using soil moisture data available from the Soil Climate Analysis Network (SCAN). The model is point based model and its performance is assessed by comparing modeled m_s to ground m_s obtained from SCAN.

This paper is organized as follows. Section II describes data used in this research. Section III presents the soil moisture model and model parameters. The comparison between estimated and observed m_s is discussed in Section IV. Finally, in section V conclusions are presented.

3.3. Data Description

This section describes the datasets used in this research. TRMMPR specifications; available volumetric soil moisture content data; and characteristics of NDVI are described. The acquisition procedure for each of the dataset is also presented.

3.4. Tropical Rainfall Measuring Mission Precipitation Radar

TRMMPR is an imaging radar aboard Tropical Rainfall Measuring Mission (TRMM) launched by NASA in December, 1997. The main objective of TRMM

satellite is to provide information on rainfall distribution in the tropical and sub-tropical regions of the world (Kummerow et al., 1998). It provides three dimensional structure of rainfall along with the information on its distribution and intensity. TRMMPR operates in *Ku*-band with HH polarization. It has a horizontal resolution of 4.4 km and cross-track scan angle between 0° and 17° with a swath width of 215 km. In August 2001, the height of TRMM satellite was increased from 350 km to 402 km to increase its mission life. This boost resulted in increase in horizontal resolution from 4.4 km to 5.0 km and swath from 215 km to 247 km for TRMM data. This has been accounted for by using the appropriate antenna footprints for the pre- and post- boost measurements.

σ° depends on dielectric constant of the area under consideration and its surface characteristics such as vegetation density and surface roughness. Dielectric constant is a measure of soil moisture content and hence can be detected by σ°. However, apart from dielectric constant, vegetation density and terrain roughness also affect σ°. It is difficult to separate the effect of vegetation density and terrain roughness.

TRMMPR orbital data is available for the tropical region lying within 36° N to 36° S. This limits the coverage to Southern US. The backscatter images of the study area are produced from this data. The images are prepared for every 14 day interval with a moving window of 7 days. Backscatter image for the study area for first 14 days of year 2000 is shown in Figure 6. The water bodies in the image are shown as white patches because of less backscatter from the smooth surface of the water body. Each pixel in the image corresponds to 4.4 km of the land surface.
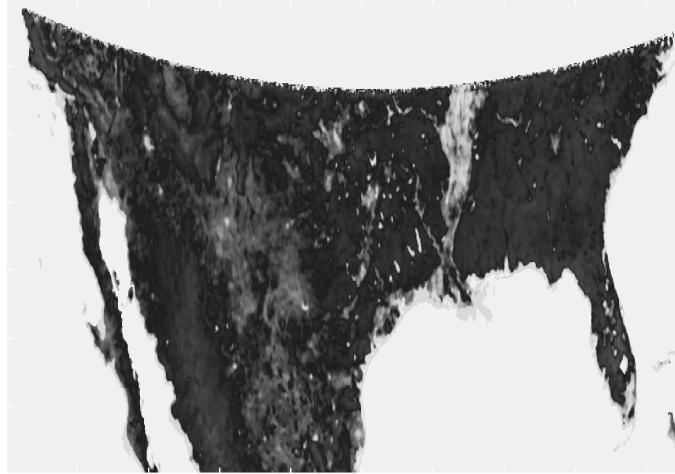
Figure 6 Backscatter image for Southern US.

3.5. Soil Moisture

The m_s data is obtained from Soil Climate Analysis Network operated by United States Department of Agriculture USDA and Natural Resources Conservation Service administered National Water and Climate Center. SCAN provides the information of various site locations across United States (US). There are currently more than 150 SCAN sites spread across US. Each site provides hourly information on various variables such as soil temperature, precipitation, and soil moisture.

There are forty seven SCAN sites in the Southern United States below 36° N latitude. These SCAN sites extend from Arizona in the west to Florida in the east covering New Mexico, Texas, Oklahoma, Arkansas, Mississippi, Alabama, Georgia and South Carolina. Figure 7 shows the spatial distribution of these SCAN sites. These sites represent diverse landuse categories. The various landuse categories, their characteristics, and the number of stations representing a given category are summarized

36

in Table 2. Although a few sites located in the western part of the region in Arizona and New Mexico, most of the sites are densely located in the Mississippi watershed where more than 80% of the landscape is covered with crop-producing fields. Some sites are spread across the south-eastern states. It is observed that the greenness of vegetation increases from west to east. This is due to the physical characteristics of the area where western region is mostly arid and semi-arid with scanty rainfall and east coast receives heavy rainfall.
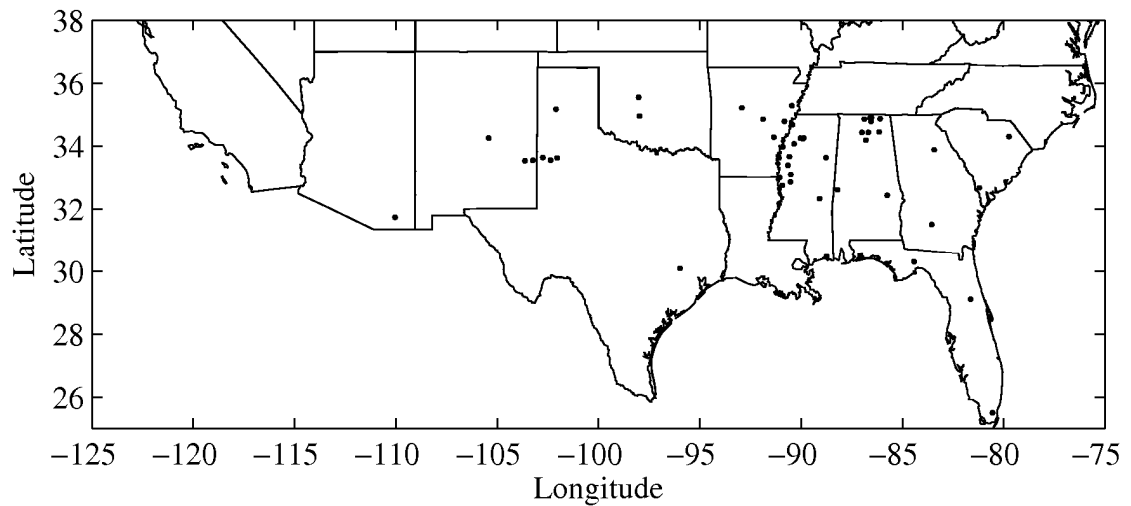
Figure 7 Spatial distribution of SCAN sites.

Table 2 Number of SCAN sites in each Landuse Category.

Landuse Category	Tree height	Canopy cover	Number of SCAN sites
Closed Shrubland	< 5 m	Bush/shrub > 40%	3
Wooded Grassland	> 5 m	10% < tree canopy < 40%	6
Grassland	-	Herbaceous cover	5
Forest	> 5 m	Canopy cover > 60%	3
Woodland	> 5 m	40% < tree canopy < 60%	7
Cropland	-	Crop producing fields	23
TOTAL			47

SCAN data consistent with the duration of time period of availability of TRMMPR data (1998-2008) is used. Each SCAN site provides hourly volumetric m_s collected by Hydra Probe II SM sensor which measures the dielectric constant of soil at depths of 5, 10, 20, 51, and 102 cm. The data corresponding to the depth of 5 cm is used in this research. The Hydra Probe is a Frequency Domain Reflectometer. It consists of capacitance plates inserted in the soil medium forming a capacitor. The capacitance changes with the change in dielectric constant of the soil medium. Hence, any changes in the soil moisture content are reflected in the capacitance. With the change in capacitance induced by the soil moisture variation, the operating frequency of the circuit varies. This frequency variation is used to measure the soil moisture by the Hydra probe sensor. The hourly soil moisture data from Hydra probe sensor at a SCAN site is averaged over 14-day period with 7-day moving window to match the data for TRMMPR $\sigma°$.

3.6. Normalized Difference Vegetation Index

NDVI is normalized difference of red band and infrared band reflectivities and is used to monitor vegetation (Tucker, 1979). It represents greenness of live vegetation in an area. It is highly correlated with other vegetation parameters like leaf area index and canopy cover and thus serves a good descriptor of vegetation discrimination (Gao et al., 2002). High values that are close to 1.0 represent forests. From the data it is observed that the low positive values from 0.2 to 0.4 indicate the presence of shrubs and grasslands and values close to zero (-0.1 to 0.1) correspond to water.

NDVI data is acquired from Earth Explorer website maintained by USGS. The 14-day NDVI composites are available for time period 1990 to 2008 at 7-day time step. The composite images are created after the removal of atmospheric effects from aerosols and water vapor that interfere with the NDVI data. Some of the images with excessive noise produced by the clouds are removed from the analysis.

3.7. Model Description

σ^o depends on soil moisture, vegetation characteristics, and surface roughness of the land surface. This section describes an empirical model that relates σ^o to the soil moisture and vegetation density (represented by NDVI). The time series of σ^o, m_s and NDVI are analyzed to develop σ°-m_s model.

σ^o is a function of several parameters given by equation 3.1.

$$\sigma^o = f\left(\lambda, \theta, p, \varepsilon, f, V\right) \qquad \text{Eqn. (3.1)}$$

39

where λ is wavelength, θ is incidence angle, p is polarization, ε is dielectric constant, f is surface roughness and V represents vegetation characteristics (FAOUN, 1989). The λ, θ, and p are radar observation parameters. Dielectric constant, surface roughness and vegetation type are land surface parameters that depend on water content in the soil, extent of corrugations on the surface and density of vegetation, respectively.

TRMMPR measurements observed in *Ku*-band are sensitive to the dielectric properties of the soil surface. Water has ε of approximately 80 whereas for dry soils ε ranges from 4 to 8. This difference in ε for water and dry soil is used as the basis for detection of m_s by σ° data.
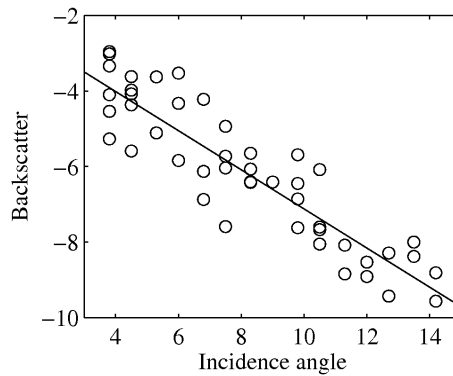
Figure 8 σ°-θ response for medium rough surface.

The σ^o measurements are affected by θ of observation. A typical σ° − θ for incidence angle range of 3 to 15 degrees is shown in Figure 8. The relationship between σ° and θ is not linear over the whole range of incidence angles. The relative contribution from surface and vegetation scattering depends on the vegetation density and is reflected

in the slope of σ°- θ response that for TRMMPR backscatter could be approximated as linear for angles between 3° and 15°. The σ°- θ is modeled as shown in equation 3.2.

$$\sigma°(\theta) = \boldsymbol{A} + \boldsymbol{B} \cdot (\theta - \theta_{ref})$$ Eqn. (3.2)

where θ_{ref} is the reference angle, **A** (dB) is the backscatter normalized to θ_{ref} and **B** (dB/°) is the slope of the line fit. θ_{ref} is chosen to be 10° at which σ° has high sensitivity to soil moisture (Ulaby et al., 1986). In this research, multiple orbit σ° measurements are used to prepare images of backscatter normalized to 10° (**A**).

The soil moisture content increases the σ^o which results in increase in **A**. **A** is also affected by the vegetation and roughness of the surface. It is difficult to decouple the effects of surface roughness and vegetation (Bindlish et al., 2003). Dense vegetation attenuates the incident electromagnetic energy and reduces the sensitivity to the underlying soil characteristics. This effect is more severe when the vegetation canopy is wet. The *Ku*-band wavelength (2.2cm) is comparable to the leaf size in the canopy and thus has higher attenuation by the canopy.

Figure 9 shows yearly variation in **A**, m_s, and NDVI at a site characterized by low NDVI. The **A** response shown in Figure 9(a) follows a seasonal pattern of highs and lows. Higher **A** values are observed in rainy and winter seasons (Aug- Dec). Lower **A** values are observed in summer months from May to Jul. The variation in soil moisture for the same duration is shown in Figure 9(b). The m_s values are higher throughout the year except for summer months from May-Jul. In summers, the soil dries through evaporation, plant consumptive use, and percolation, thus reducing the backscatter. The

backscatter contribution in this case is mainly from the geometrical characteristics of the surface. From both the figures it is seen that the m_s behavior is well captured by **A** values. The intermittent highs and lows in m_s from Aug-Dec are also seen in **A** response. The scatterplot of **A** values and m_s is shown in Figure 9(d). A high correlation of 0.79 shows the ability of **A** to capture m_s values.

The variation in NDVI for the same site and same duration is shown in Figure 9(c). Typical NDVI values in this site (0.3-0.45) represent croplands. The peak in the NDVI values is observed in the months of May and Aug. NDVI variation is reflected in A response with correlation of 0.42 between **A** and NDVI as shown in Figure 9(e).
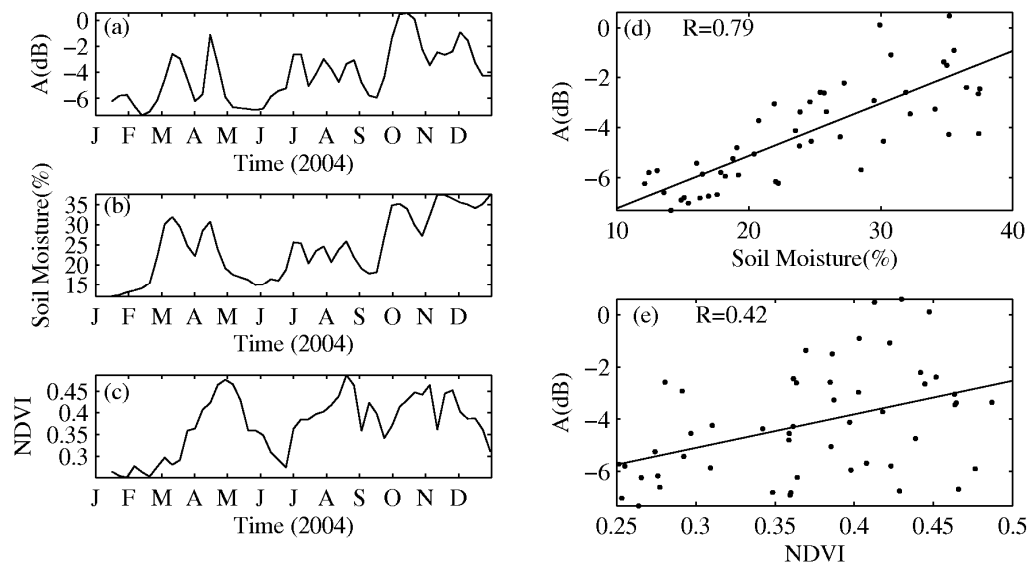
Figure 9 Time series plot of (a) A, (b) Soil Moisture, and (c) NDVI at site with low NDVI. (d) Scatterplot of A and m_s, and (e) Scatterplot between A and NDVI.
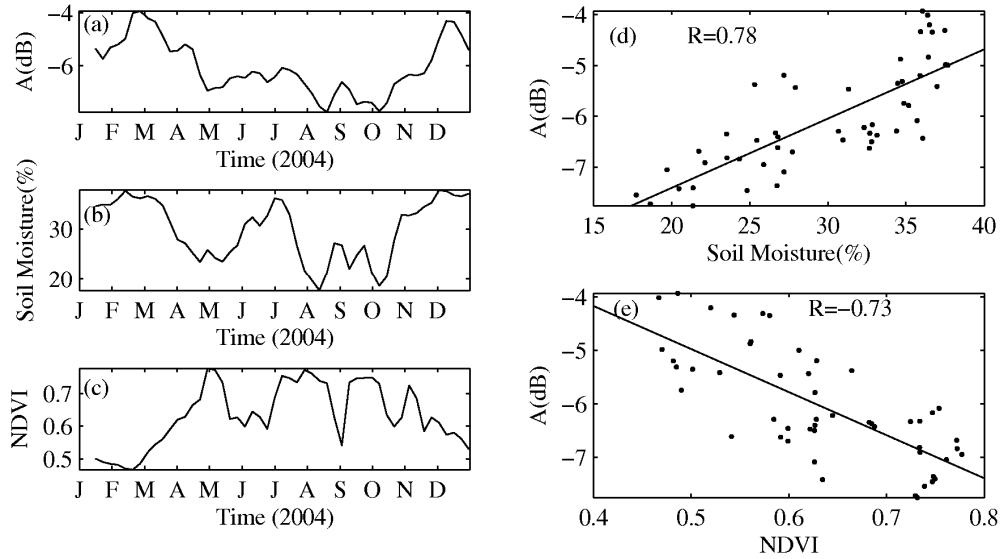
Figure 10 Time series plot of (a) A, (b) Soil Moisture, and (c) NDVI at site with high NDVI. (d) Scatterplot of A with m_s, and (e) Scatterplot between A and NDVI.

The annual behavior of **A**, m_s, and NDVI for a site characterized by high vegetation is shown in Figure 10. The time series of **A** and m_s is shown in Figure 10(a) and Figure 10(b), respectively. It is seen that the **A** response follows the variation in m_s. Both **A** and m_s show high values throughout the year except for the months May, Aug, and Oct. The scatterplot of **A** and m_s reveals a high correlation of 0.78 between **A** and m_s. However, NDVI variation shown in Figure 10(c) shows the variation in NDVI opposite to **A** response of the site. This is due to the high average values of NDVI (0.5-0.8) representing dense vegetation. In case of dense vegetation, the backscatter gets attenuated by the leaves of the vegetation which reduces the penetration depth of incident waves. A negative correlation of -0.73 between **A** and NDVI is observed and shown in Figure 10(e).

43

3.8. Soil Moisture Model

The soil moisture model expresses m_s in terms of **A** and normalized NDVI. **A** captures the backscatter of the land surface that represents the dielectric nature of the surface and vegetation characteristics above it. The vegetation on the land surface is represented by NDVI. Low vegetated areas have low NDVI values whereas; highly vegetated areas are represented by high NDVI values. m_s is related to **A** and NDVI as shown in equation 3.3.

$$m_s(A, NDVI) = \boldsymbol{\mu_s} + \mathbf{T} \cdot A + \mathbf{P} \cdot (NDVI - \mu_{ndvi}) \qquad \text{Eqn. (3.3)}$$

where, m_s is soil moisture in %, **A** is backscatter measured in decibels (dB) normalized to 10° and NDVI is a unitless index with μ_{ndvi} being the average value of NDVI over the training period. $\boldsymbol{\mu_s}$ denotes the modeled average value of soil moisture for a SCAN site under consideration. **T** and **P** are the weights of **A** and NDVI, respectively, and represent the dependence of modeled soil moisture on **A** and NDVI, respectively. $\boldsymbol{\mu_s}$, **T**, and **P** are the calibration parameters in (%), (%/dB), and (%), respectively.

3.9. Calibration and Validation

The calibration of the model aims at obtaining the model parameters– $\boldsymbol{\mu_s}$, **T**, and **P**. m_s, **A** and NDVI data over a given SCAN site are used to compute the model parameters by minimizing the error to obtain m_s from **A** and NDVI. The model is calibrated using 75% of the time series data and model parameters $\boldsymbol{\mu_s}$, **T**, and **P** are computed. These model parameters are then used to estimate m_s for the remaining 25%

of the data. The validation is performed by comparing the m_s values obtained from the model with the observed m_s values. The correlation coefficient (R), root mean square error (rmse), and mean absolute error (mae) are computed between observed and modeled soil moisture and the accuracy of the model is assessed.

3.10. Results and Discussions

The soil moisture model is applied to all the SCAN sites in Southern US and the sites are grouped on the basis of their landuse type to assess the behavior of the model on individual landuse. The ensuing figures show a time series plot of observed and modeled soil moisture, scatterplot, and non-exceedance probability plot for representative sites for each landuse. The ensemble plots of scatterplot, non exceedance probability, and boxplot distribution for observed and modeled soil moisture for all the sites in a given landuse are also shown.

The model results for sites in woodland are shown in Figure 11. Woodland is land where tree heights exceed 15 ft and tree canopy cover lies between 40% and 60%. Figure 11(a) shows the time-series plot of observed m_s and modeled m_s for 2 years of testing data at a representative site of woodland. The modeled values of m_s compare well with the observed values of m_s. The peaks in the time series of m_s are introduced by events of rainfall that increase the soil water content in the soil. After a rainfall event, the soil moisture is lowered due to the process of evaporation, evapo-transpiration, and vegetation growth. These highs and lows in the soil moisture are well captured by the

45

model. Figure 11(b) shows the scatterplot between observed and modeled m_s. The points that are located above the bisector line indicate over-estimation of soil moisture whereas points that fall below the line are under-estimated values of soil moisture. The model works reasonably well with R=0.81 and RMSE=4.16%. It is seen in Figure 11(b) that the model over-estimates the m_s where observed m_s is below 30% and under-estimates the m_s for observed m_s values that are above 30%. Figure 11(c) shows the plot of probability of non-exceedance of error. The plot shows the percentage of the data samples as a function of the probability of their absolute modeling error on the y-axis being less than or equal to the values on the x-axis. According to the plot, 79% of the data points have an error of 5% or less which increases to 99.7% of the data points having an error of 10% or less.

Figure 11(d-f) shows the ensemble plots for the combined model performance of all 7 woodland sites. The sites in this area are densely vegetated (NDVI ranges from 0.59 to 0.71) and have varying degrees of soil moisture ranging from 1.2% to 40.9%. The model results for woodland sites show promising results. Figure 11(d) shows the saturation of all the data points for sites located in woodland along the 45° line with high correlation 0.89 and root mean square error of 5.0%. Figure 11(e) shows the non-exceedance probability plot which reveals that 74% of the soil moisture estimates have an error of 5% and less whereas, 95% of the estimates has 10% or less error. Figure 11(f) compares the distributions of modeled and observed soil moisture using boxplot. The boxplot describes the median of both the datasets as the horizontal line in the box.

46

The 25th and 75th percentile of the data is defined by the lower and upper bounds of the box, respectively. The whisker at the lower end of the data is 5th percentile whereas whisker at the upper end is 95th percentile. It can be seen from the boxplot that the majority of the values, lying within the box of 25th and 75th percentile match well between observed and modeled soil moisture. However, the modeled m_s is unable to capture very dry values (close to zero) that are seen in the distribution of observed m_s. The model also does not work well in the wet conditions since the model over-estimates the m_s values for high observations close to 40%.

Figure 11 Model results for Woodland. (a) Time series plot for observed and modeled soil moisture. (b) Scatterplot of observed and modeled soil moisture. (c) Non-exceedance probability curve of mean absolute error. (d) Scatterplot of all SCAN sites that lie in Woodland. (e) Non-exceedance probability plot of mean absolute error of all the SCAN sites that lie in Woodland. (f) Box-plot of the observed and modeled soil moisture for the data points in the group.

A similar analysis is performed over wooded grassland and the results are shown in Figure 12. Wooded grassland is characterized by high NDVI values from 0.59 to 0.67 indicating dense vegetation. However, the tree canopy cover for wooded grassland is lesser than woodland and lies between 10% and 40%. The tree heights in wooded grassland exceed 15 ft as in woodland. It has varying degree of m_s ranging from 1.4% to 42.5%. Figure 12(a) shows the time series plot between observed and modeled soil moisture for 3 years of testing data at a representative site of wooded grassland. The beginning of the year 2006, 2007, and 2008 show that the model under-estimates the m_s values. This under-estimation of the points is also reflected in Figure 12(b) where most of the points lie below the 45° line. Root mean square error is 6.8% and correlation is 0.75. The non-exceedance probability curve in Figure 12(c) shows that 88% of the soil moisture estimates have an error of 10% or less.

The combined results of the model applied to 6 wooded grassland sites are shown in Figure 12(d-f). Relatively more data points fall below the 45° line as shown in Figure 12(d). The non-exceedance probability plot in Figure 12(e) reveals that the model gives a 10% or less error for 94% of the estimates. The boxplot distribution in Figure 12(f) reveals that unlike woodland, where the model does not capture the m_s values close to 40%, in wooded grassland, the 95th percentile and 75th percentile of modeled and observed m_s match with each other quite well.

Figure 12 Model results for Wooded Grasslands. (a) Time series plot for observed and modeled soil moisture. (b) Scatterplot of observed and modeled soil moisture. (c) Non-exceedance probability curve of mean absolute error. (d) Scatterplot of all SCAN sites that lie in Wooded Grassland. (e) Non-exceedance probability plot of mean absolute error of all the SCAN sites that lie in Wooded Grassland. (f) Box-plot of the observed and modeled soil moisture for the data points in the group.

The performance of the model in the area of grassland is shown in Figure 13. Grassland is covered with continuous herbaceous cover consisting of less than 10% tree canopy cover. Figure 13(a) shows the variation between observed and modeled soil moisture values for 2 years of testing period. The model works well and has captured the variation in soil moisture well. However, the model is unable to represent the decrease in soil moisture observed in the middle of the year (summer) 2007 and 2008. The data points in Figure 13(b) are saturated near the 45° line indicating a good performance of the model. Model performance parameters for the site are R=0.80 and root mean square error=7.8%. This high error in root mean square error is attributed to the inability of the model to describe the low soil moisture values observed at the site.

49

The non-exceedance probability plot in Figure 13(c) shows that 45% of the data has 5% or less error in the soil moisture estimates which increases to 10% or less error for 80% of the estimates.

The combined result of applicability of model to all the 5 sites in grassland is summarized in Figure 13(d-f). The sites in grassland have large extent of variability in terms of average soil moisture content. Soil moisture values lie between 0.4% and 43.6%. The NDVI values in grassland are low and range from 0.26 to 0.33 except for two points where it in the range from 0.58 to 0.63. Figure 13(d) shows the scatterplot of observed and modeled soil moisture for all grassland sites. Unlike woodland, the model works well at m_s values close to 40%. Figure 13(e) shows the non-exceedance probability plot for grassland. It can be inferred from the figure that 95% of the soil moisture estimates have an error of 10% or less. The modeled soil moisture data points in box-plot are shown in Figure 13(f). Except for the extremely low soil moisture values, the model is able to estimate observed soil moisture well.
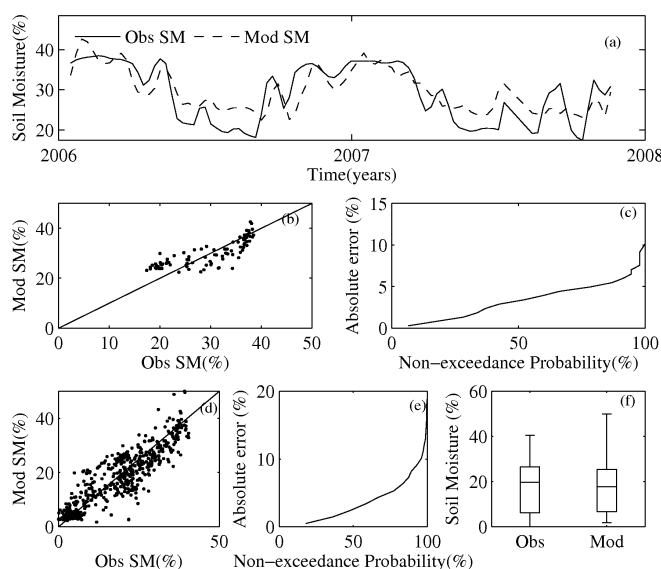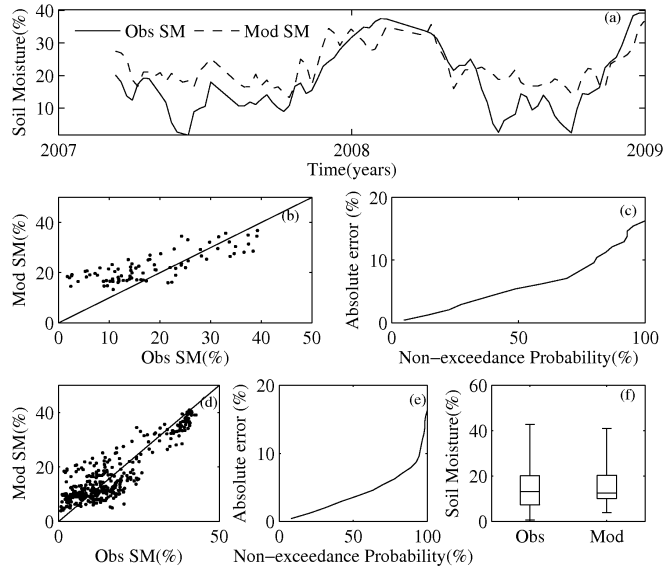
Figure 13 Model results for Grassland. (a) Time series plot for observed and modeled soil moisture. (b) Scatterplot of observed and modeled soil moisture. (c) Non-exceedance probability curve of mean absolute error. (d) Scatterplot of all SCAN sites that lie in Grassland. (e) Non-exceedance probability plot of mean absolute error of all the SCAN sites that lie in Grassland. (f) Box-plot of the observed and modeled soil moisture for the data points in the group.

The Great Plains of Southern US consists of extended croplands where more than 80% of the land is covered by crop producing plants. Almost half of the SCAN sites studied in this research lie in croplands. A representative site in cropland is shown in Figure 14(a-c). The model works well at this site with R=0.71 and root mean square error=4.0%. Most of the data points at this site are under-estimated. The non-exceedance probability plot in Figure 14(c) shows that 96% of the data points have an error of 10% or less.

The model results for a combined analysis of all the 23 cropland sites are shown in Figure 14(d-f). Figure 14(d) shows the scatterplot of observed and modeled soil moisture. The majority of the points are along the 45° line with some over-estimation in

51

drier conditions of soil moisture. The absolute error non-exceedance probability curve is shown in Figure 14(e). The plot shows that 69% of the estimates have an error of 5% or less which increases to 10% or less for 90% of the estimates. The distribution of observed and modeled m_s is shown in Figure 14(f). The modeled soil moisture captures the median and 75th percentile of data points very well. The wide spatial distribution of 23 sites spread across Southern US with varying degree of NDVI values and soil moisture contents is the reason for 10% or less error for 90% of the estimates.
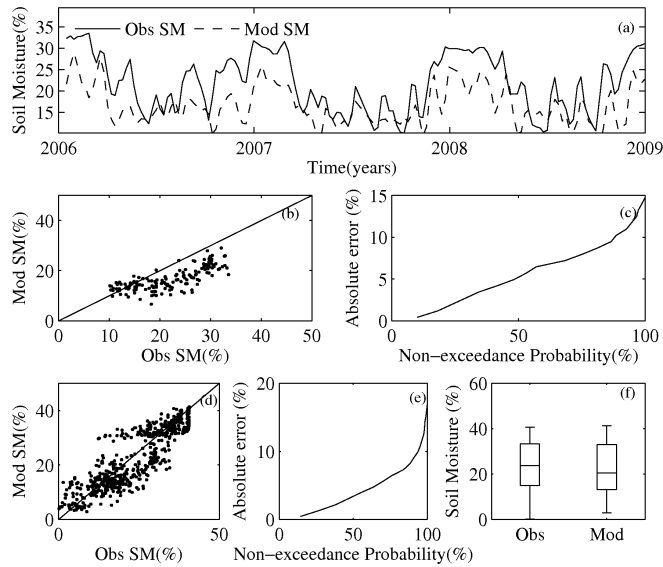

Figure 14 Model results for Cropland. (a) Time series plot for observed and modeled soil moisture. (b) Scatterplot of observed and modeled soil moisture. (c) Non-exceedance probability curve of mean absolute error. (d) Scatterplot of all SCAN sites that lie in Cropland. (e) Non-exceedance probability plot of mean absolute error of all the SCAN sites that lie in Cropland. (f) Box-plot of the observed and modeled soil moisture for the data points in the group.

The model results for sites in closed shrubland are shown in Figure 15. Closed shrubland is land covered with shrubs. The shrubs do not increase more than 15 ft in

52

height. Closed shrubland sites lie in the western part of Southern US that comprises of arid and semi-arid regions and are characterized by low soil moisture throughout the year with average soil moisture ranging from 4.8% to 6.2% and low NDVI values from 0.29 to 0.35. The modeled soil moisture compares well with observed soil moisture as seen in Figure 15(a). The representative site is dry with m_s values less than 20%. The model works well with R=0.60 and root mean square error=3.52%. The plot for the site in Figure 15(c) shows that all the data points at the site have an absolute error of less than 8%.

Figure 15(d-f) shows the combined model performance of all the 3 sites that lie in closed shrubland. The relative dryness of the area is seen in Figure 15(d). The soil moisture does not increase more than 20% at any time of the year for any site. The non-exceedance probability plot for these sites is shown in Figure 15(e). According to the plot, 84% of the data points have an error of 5% or less and 100% of the data points having less than 8% error. Figure 15(f) compares the distributions of modeled and observed soil moisture using boxplot. It is seen that the model does not perform well in extreme dry situations.
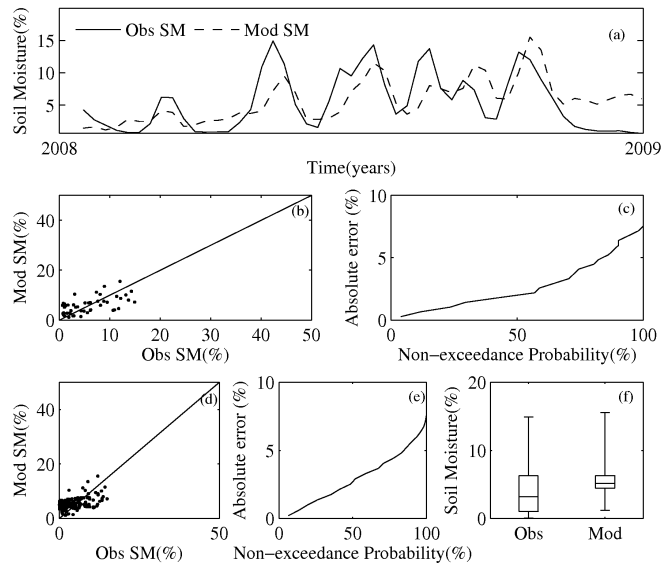
Figure 15 Model results for Closed Shrubland. (a) Time series plot for observed and modeled soil moisture at a representative site. (b) Scatterplot of observed and modeled soil moisture at a representative site. (c) Non-exceedance probability curve of mean absolute error at a representative site. (d) Scatterplot of group of SCAN sites that lie in Closed Shrubland. (e) Non-exceedance probability plot of mean absolute error of group of sites that lie in Closed Shrubland. (f) Box-plot of the observed and modeled soil moisture for the data points in the group.

Model results for sites in the forest (deciduous + mixed) are shown in Figure 16. Figure 16(a) shows the temporal variation of soil moisture for observed and modeled soil moisture for 2 years of testing data. Though the model compares well, it performs poorly where soil moisture drops to low values. This over-estimation of the low soil moisture values is indicated in Figure 16(b) where most of the points fall above the 45° line. The non-exceedance probability plot shows that 91% of the estimates have an error of 10% or less.

For combined group results, the model works well in forested areas as well. Figure 16(f) shows the box-plot of the modeled and observed soil moisture data points.

The distributions of observed and modeled m_s show that the model is able to capture the overall behavior of the soil moisture in the region. The non-exceedance probability curve shown in Figure 16(e) describes that 69% of the estimates show an error of less than 5% which increases to 92% of the estimates that show an error of 10% or less.
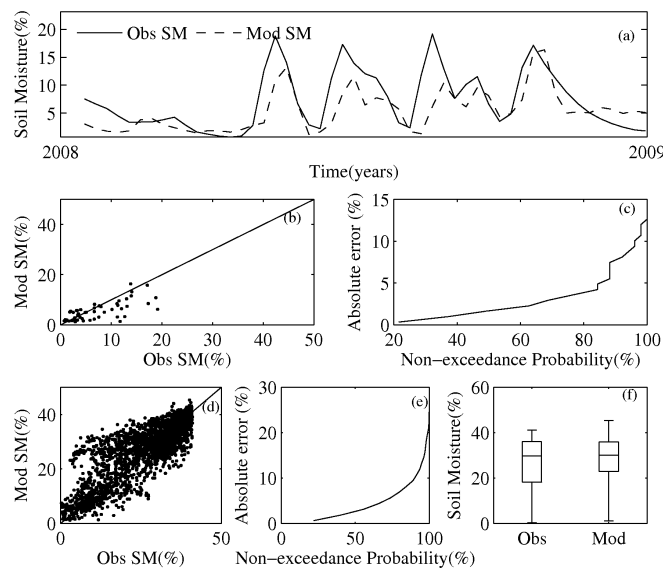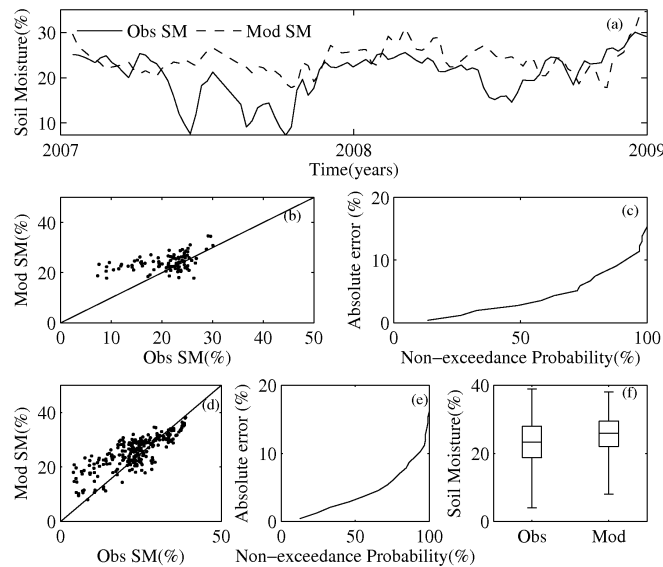

Figure 16 Model results for Forest. (a) Time series plot for observed and modeled soil moisture. (b) Scatterplot of observed and modeled soil moisture. (c) Non-exceedance probability curve of mean absolute error. (d) Scatterplot of all SCAN sites that lie in Deciduous Forest. (e) Non-exceedance probability plot of mean absolute error of all the SCAN sites that lie in Deciduous Forest. (f) Box-plot of the observed and modeled soil moisture for the data points in the group.

The model relates soil moisture to TRMMPR backscatter measurements and NDVI quite well over diverse type of landuse. A summary of the model results for sites comprising each landuse across the Southern US is listed in Table 3. The model works best for woodland. For landuse characterized by dense vegetation, the performance of the model decreases due to attenuation of incident microwave radiations by the

55

vegetation canopy leaves. The dense vegetation canopy causes volume scattering of incident wave and thus results in lesser contribution from the underlying soil surface. It is observed that the model does not work well at low soil moisture values. With the exception of woodland for which the model over-estimates the high m_s values close to 40%, the model works well over high m_s values in other landuse types.

Table 3 Summary of model statistics for each landuse.

Landuse	Number of sites	R	rmse	Percentage of estimates with error < 5%	Percentage of estimates with error < 10%
Woodland	7	0.89	5.0%	74%	95%
Wooded Grassland	6	0.86	5.6%	65%	94%
Grassland	5	0.88	5.5%	66%	95%
Cropland	23	0.83	6.3%	69%	90%
Closed Shrubland	3	0.45	3.5%	84%	100%
Forest	3	0.79	5.6%	69%	93%

3.11. Conclusions

A simple linear model that relates soil moisture to TRMMPR backscatter measurements is presented. The dielectrical constant of the land surface affects backscatter and is used to measure water content of the soil. The physical properties of the land surface that affect backscatter are surface roughness, topography, and vegetation cover. The vegetation cover in the model is accounted for by using NDVI. The effects of surface roughness and topography are not taken into account. The model performs well and is able to estimate the soil moisture values reasonably well.

The model works well in woodland, wooded grassland, and grassland where the combined correlation for all the data points is 0.89, 0.86, and 0.88, respectively. The non-exceedance probability plot for these three landuse types reveals that 95% of the estimates have an error of 10% or less which is a good measure of the model performance. The model works best for closed shrubland for which the non-exceedance probability plot shows that 100% of the soil moisture estimates have 10% or less error. This is because the closed shrubland sites are mainly located in the arid western part of the Southern US. This area is characterized by bare ground or scanty vegetation. The incident radiation penetrates through the vegetation canopy cover and provides backscatter from underlying surface.

This research provides an alternate method of measuring soil moisture. The method provides an alternative to installation of measurement instruments at each site and provides the soil moisture measurements over a wide extent of land. This research provides an insight into measurement of soil moisture using space-borne remote sensing. The research can help scientists, engineers, and policy-makers to understand the comprehensive spatial and temporal variability of soil moisture without having the need to measure soil moisture at individual sites. Soil moisture measurements over a large extent of area can provide the opportunity to understand various hydrologic processes and manage scarce water resources in an efficient manner.

3.12. References

Bindlish, R., Jackson, T. J., Wood, E., Gao, H. L., Starks, P., Bosch, D., et al. (2003). Soil moisture estimates from TRMM Microwave Imager observations over the Southern United States. Remote Sensing of Environment, 85(4), 507-515.

Das, N. N., & Mohanty, B. P. (2006). Root zone soil moisture assessment using remote sensing and vadose zone modeling. Vadose Zone Journal, 5(1), 296-307.

Das, N. N., Mohanty, B. P., Cosh, M. H., & Jackson, T. J. (2008). Modeling and assimilation of root zone soil moisture using remote sensing observations in Walnut Gulch Watershed during SMEX04. Remote Sensing of Environment, 112(2), 415-429.

Gao, H., Wood, E. F., Jackson, T. J., Drusch, M., & Bindlish, R. (2006). Using TRMM/TMI to retrieve surface soil moisture over the southern United States from 1998 to 2002. Journal of Hydrometeorology, 7(1), 23-38.

Houser, P. R., Shuttleworth, W. J., Famiglietti, J. S., Gupta, H. V., Syed, K. H., & Goodrich, D. C. (1998). Integration of soil moisture remote sensing and hydrologic modeling using data assimilation. Water Resources Research, 34(12), 3405-3420.

Jackson, T. J. (1993). Measuring Surface Soil-Moisture Using Passive Microwave Remote-Sensing .3. Hydrological Processes, 7(2), 139-152.

Kummerow, C., Barnes, W., Kozu, T., Shiue, J., & Simpson, J. (1998). The Tropical Rainfall Measuring Mission (TRMM) sensor package. Journal of Atmospheric and Oceanic Technology, 15(3), 809-817.

Nations, U. (1989). Microwave remote sensing handbook. Rome, Italy: European Space Agency.

Oki, T., Seto, S., & Musiake, K. (2000). Land surface monitoring by backscattering coefficient from TRMM/PR 2A21. Paper presented at the Geoscience and Remote Sensing Symposium, 2000. Proceedings. IGARSS 2000. IEEE 2000 International.

Schneider, K., Huisman, J. A., Breuer, L., Zhao, Y., & Frede, H. G. (2008). Temporal stability of soil moisture in various semi-arid steppe ecosystems and its application in remote sensing. Journal of Hydrology, 359(1-2), 16-29.

Song, D. S., Zhao, K., & Guan, Z. (2007). Advances in research on soil moisture by microwave remote sensing in China. Chinese Geographical Science, 17(2), 186-191.

Su, Z. B., Yacob, A., Wen, J., Roerink, G., He, Y. B., Gao, B. H., et al. (2003). Assessing relative soil moisture with remote sensing data: theory, experimental validation, and application to drought monitoring over the North China Plain. Physics and Chemistry of the Earth, 28(1-3), 89-101.

Tucker, C. J. (1979). Red and Photographic Infrared Linear Combinations for Monitoring Vegetation. Remote Sensing of Environment, 8(2), 127-150.

Verhoest, N. E. C., Troch, P. A., Paniconi, C., & De Troch, F. P. (1998). Mapping Basin Scale Variable Source Areas From Multitemporal Remotely Sensed Observations of Soil Moisture Behavior. Water Resour. Res., 34.

Wagner, W., Scipal, K., Pathe, C., Gerten, D., Lucht, W., & Rudolf, B. (2003). Evaluation of the agreement between the first global remotely sensed soil moisture data with model and precipitation data. Journal of Geophysical Research-Atmospheres, 108(D19), -.

Wigneron, J. P., Schmugge, T., Chanzy, A., Calvet, J. C., & Kerr, Y. (1998). Use of passive microwave remote sensing to monitor soil moisture. Agronomie, 18(1), 27-43.

CHAPTER 4

ESTIMATION OF WATER STAGE OVER WETLANDS OF SOUTH FLORIDA

USING TRMMPR OBSERVATIONS

4.1.   Abstract

Everglades are a critical component of the regional hydrological cycle in South Florida. Anthropogenic activities in this region have deteriorated the wetland ecosystem and efforts are on-going to restore and preserve it. Seasonal and interannual changes in water stage result in saltwater intrusion and inhibit ecosystem conservation measures. Hence, there is a need to monitor water stage in wetlands. Microwave remote sensing with its sensitivity to surface characteristics provides an opportunity to measure changes in water stage from space. Space-borne remotely sensed data can provide a comprehensive spatio-temporal distribution of water stage over an area thereby eliminating the need to monitor water stage separately at each measurement site.

This research relates water stage measurements (w_s) to Tropical Rainfall Measuring Mission Precipitation Radar backscatter ($\sigma°$). $\sigma°$ response to partially exposed vegetation is used as the basis of the model. Variations in the water depth change the amount of exposed vegetation canopy that is reflected in the $\sigma°$ measurements. An empirical linear model is developed that expresses w_s in terms of $\sigma°$. The impact of vegetation on the model is studied by examining model performance over various landcovers.

The w_s-model is applied to stage data on 114 sites operated by South Florida Water Management District. Eleven year data (1998 to 2008) is used for this research. The model is calibrated using 75% of the time period of data to estimate the model parameters; and validated over the remaining 25% of the time period.

The estimated water stage measurements from the model are compared with observed measurements for various landcovers. The model performance is assessed by comparing correlation coefficient (R), root mean square error (rmse), and non-exceedance probability of difference between observed and modeled water stage measurements. The model works reasonably well in the regions with tree heights greater than 15 ft e.g., over woodlands, R=0.98 and rmse=0.64 ft. Other relatively shorter height vegetation landcovers such as cropland (R=0.90, rmse=0.60 ft) and grassland (R=0.97, rmse=0.66 ft) also exhibit reasonable performance of the model. The model performance is linked to the vegetation features with varying submergence from changes in water stage. Thus, microwave remote sensing signal over partially inundated vegetation can provide spatio-temporal characteristics of water stage. This research provides a new insight into measurement of water stage using spaceborne remote sensing techniques.

4.2.   Introduction

South Florida contains thousands of lakes and swamps. 1.2 million hectares of South Florida consists of wetlands (Doren et al., 1999). Wetland is an area where the

soil is saturated seasonally or perennially resulting in shallow pools of standing waters. Wetlands support rich biodiversity of endangered and threatened species (Kushlan et al., 1990; Fennema et al., 1994). Plant life and communities found in the wetlands consists of mangroves, water lilies, cypress, and gum whereas animal life comprises of various amphibians, reptiles, birds and furbearers. The study of wetlands is termed as Paludology (Gotkiewicz, 2005) which is of significant interest to scientists, biologists, and environmentalists.

Existence of wetlands in South Florida region is beneficial through improved water quality, and recharging of the ground aquifer (Daily et al., 1997). Wetlands have the ability to store floodwater and protect shoreline (Brande 1980). These wetlands are hydrologically closed and play an important role in flood control, contaminant attenuation, and carbon sequestration (McAllister et al., 2000; Pant et al., 2003). These wetland play an important role in the regional ecology and hydrological cycle.

Understanding hydrological phenomenon in wetland is of utmost importance as it helps in maintaining ecological functions and protecting economic benefits of the region (Ozesmi and Bauer, 2002). The water bodies and lakes in South Florida experience significant changes in the seasonal and interannual cycle of water stage because of highly variable climate. It is important to understand the changes in water stage as it alters the water flow path between surface and ground water (Johnson et al., 2004). Saltwater intrusion is a result of excessive decrease in water stage where salty sea water flows into the wetland ecosystem. Water stage variability is the chief cause of

changes in salinity in the wetlands (Gorham et al., 1983) which modifies the vegetation patterns in the region. Any change in the vegetation patterns of wetlands affect the food supply and nesting patterns of waterfowl (Covich et al., 1997). Hence, there is a need to monitor water stage in wetlands. However, due to wide expanse of geologically complex wetlands and lack of hydrological surveys, most of the lakes especially small lakes are barely monitored (Zhang, 2008). Moreover, most of the water stages measuring stations in South Florida are placed near water control structures which do not provide much insight into the water level variations in the wetlands. Hence, there is a need to obtain a comprehensive spatio-temporal distribution of water stage using an alternative method.

Tropical Rainfall Measuring Mission (TRMM) Precipitation Radar (TRMMPR) has been observing land surface backscatter ($\sigma°$) since 1998. $\sigma°$ is sensitive to dielectric and physical characteristics of the target area which is mostly attributed to the water content and vegetation, respectively of the target area. Over standing water, smooth surface results in specular reflection of the incident radiations resulting in very low backscatter. On the other hand, backscatter from partially inundated vegetation is dependent on the physical characteristics of the canopy exposed above water. The density of vegetation exposed above the water surface is related to backscatter from the surface.

In this paper, a research is conducted to estimate water stage (w_s) measurements using space-borne remote sensing. A model is developed that relates w_s measurements to

TRMMPR *Ku*-band (wavelength of 2.2 cm) backscatter. This backscatter depends on the volume scattering characteristics of exposed vegetation. The effect of vegetation on model performance is investigated by incorporating into the model, the Normalized Difference Vegetation Index (NDVI) as a measure of greenness of the vegetation.

This paper is organized as follows. Section II describes the study area. This is followed by data description in Section III. Section IV presents the w_s model and model parameters. The comparison between estimated and observed w_s is discussed in Section V. Finally, in section VI conclusions are presented.

4.3. Study Area

Geographically, South Florida is defined by water since it is surrounded by Atlantic Ocean on one side (east) and Gulf of Mexico on the other two sides (west and south). It consists of thousands of small lakes and other water bodies. The largest lake in the region is Lake Okeechobee that occupies 730 square miles of the area. It is a shallow lake with average depth of 9 feet. Generally lake levels are maintained between 13 to 15 feet of National Geodetic Vertical Datum (NGVD).

The Everglades Agricultural Area (EAA) lies to the immediate south of the Lake Okeechobee. Many canals run through the EAA originating from the Lake Okeechobee to the Atlantic Ocean as shown in Figure 17. Adjacent to EAA are the Water Conservation Areas (WCAs) that store the surplus water in the region. This region has a large number of manmade levees and water control structures. There is a complex

64

interaction between manmade and natural features in this region. Everglades National Park that lies to the west of WCAs is covered mainly with the tropical and sub-tropical forests and preserver the natural environment of Everglades.

The South Florida region is characterized by heavy rainfall of about 4-5 ft/yr that results in large volumes of surface water. Most of this water evaporates, infiltrates or drains to the ocean. One of the major economic resources of the region is agriculture that is abundant in the interiors of South Florida. The climate of South Florida is favorable to a variety of crops throughout the year. Sugarcane and citrus fruits are the major agricultural produce of the region. These large scale agricultural practices in South Florida started in 1920 after draining large volumes of peat soil from the region. This increased the agricultural water demand in the region. This water demand was further increased with growing human population in the surrounding areas of Lower East Coast.

South Florida faces a common problem of saltwater intrusion. The region consists of various canals that drain from interiors of South Florida to nearby Gulf of Mexico or Atlantic Ocean. These canals lower the water table causing the intrusion of seawater. During dry season and periods of drought, the seawater moves inland through the canals and infiltrates into the aquifers. Lowering of ground water table creates a negative head and allows the seepage of saltwater into the aquifers. However, the problem of uncontrolled saltwater intrusion has been addressed by construction of various control structures near the outlets of the drainage canals. These controls are

opened to release excess of water during rainy seasons to avoid flooding in the region. During the dry season, control gates are closed to prevent the intrusion of seawater through canals. South Florida Water Management District (SFWMD) is a government agency that operates the water control structures in South Florida to prevent flooding and regulate the water flow. In certain areas, mainly WCAs the operation of the flood control structures result in the accumulation of water in excess of natural background levels (Wdowinski et al., 2008). Therefore, it becomes important to monitor water stage in order to understand the hydrological flow in wetlands.
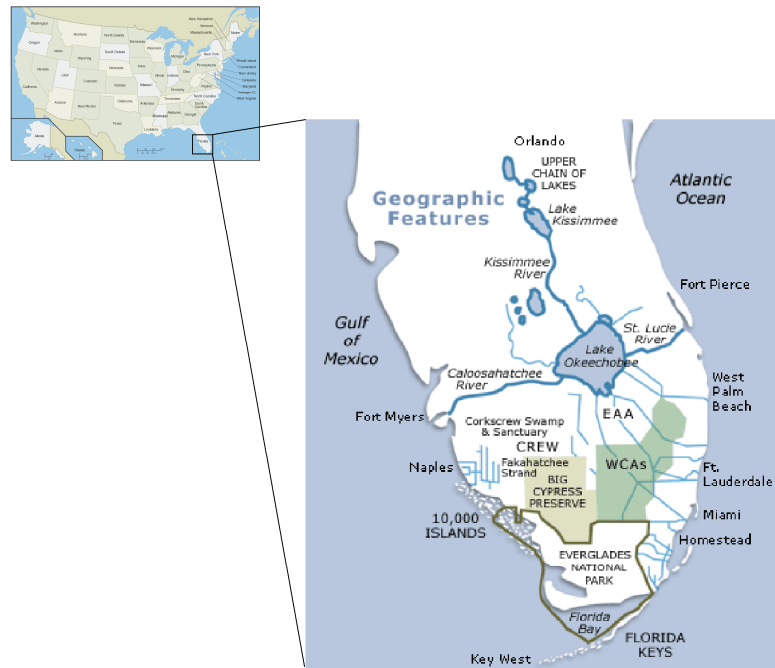
Figure 17 Geographical features of South Florida (Source: SFWMD website).

There are 804 SFWMD stage measuring sites in South Florida. However, 115 sites that lie in the wetland regions of ENP, WCAs, and Big Cypress are selected for study. The

66

location of these sites is shown in Figure 18. Out of these 123 sites, 45 of them are

located in WCAs, 41 lie in ENP, and 37 lie in Big cypress.
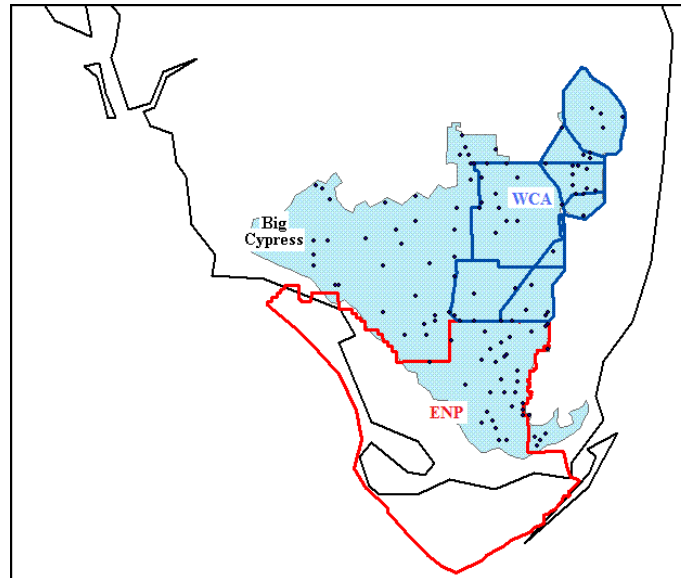
Figure 18 SFWMD Stage measuring sites in the study areas- ENP, WCAs, and Big
Cypress.

4.4.   Data Description

This section describes the datasets used in this research. The Tropical Rainfall

Measuring Mission (TRMM) specifications, measurement of water stage and

characteristics of Normalized Difference Vegetation Index (NDVI) are described. The

acquisition procedure for each of the dataset is also presented.

4.5.   Tropical Rainfall Measuring Mission Precipitation Radar

The main objective of TRMM satellite is to provide information on rainfall

distribution in the tropical and sub-tropical regions of the world (Kummerow et al.,

1998). It provides three dimensional structure of rainfall along with the information on its distribution and intensity. TRMMPR operates in *Ku*-band with HH polarization. It has a horizontal resolution of 4.3 km and cross-track scan angle scanning between 0° and 17° with a swath width of 215 km. In August 2001, the height of TRMM satellite was increased from 350 km to 402 km to increase the mission life. This boost resulted in increase in horizontal resolution from 4.3 km to 5.0 km and swath from 215 km to 247 km for TRMM data. This change has been accounted for in the computation of σ° by changing the antenna footprints accordingly.

Figure 19 shows the conceptual behavior of TRMMPR incident radiation over inundated areas with exposed and submerged vegetation. σ° depends on the amount of the partial submergence of vegetation. In the areas with high water stage (submerged vegetation), the water surface is typically smooth which results in specular reflection of the incident radiation from TRMMPR. The specular reflection results in low or no backscatter. It is noted that for nadir (vertical) view, i.e. θ=0° (not considered in this research), the specular reflection would be directed back to the sensor. In the areas where height of vegetation is greater than the water stage, the backscatter signal depends on the amount of submergence of vegetation. This principle is used in the research to estimate the effect of water stage on σ° measurements.
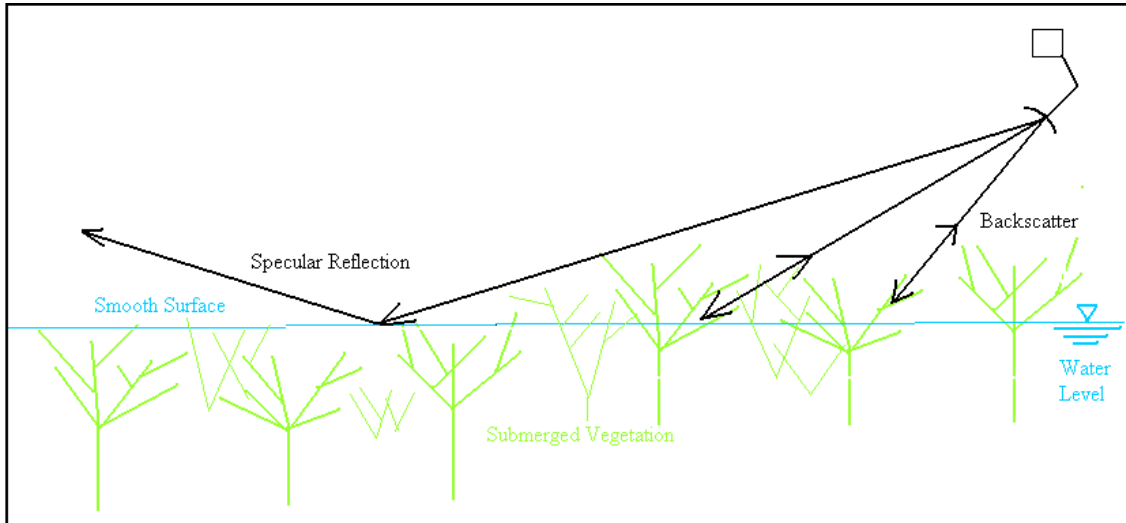
Figure 19 Behavior of TRMMPR incident radiation over inundated areas.

TRMMPR orbital data is available for the tropical region lying within 36° N to 36° S. The images of the study area are produced from this data for 14 day intervals with a moving window of 7 days. Each pixel in the image corresponds to 2 km of the land surface.

4.6. Water Stage

w_s data is obtained from South Florida Water Management District (SFWMD) database DBHYDRO. SFWMD provides the information of various site locations across South Florida. There are currently more than 700 water stage measuring sites spread across Southern Florida. Each site provides daily information on various variables such as precipitation and water stage.

The data from SFWMD's database DBHYDRO sites is obtained for eleven years from 1998 to 2008. The hourly water stage measurement at a site is averaged over 14-

69

day period with 7-day moving window to match the temporal resolution of the TRMMPR backscatter.

4.7.   Normalized Difference Vegetation Index

NDVI is normalized difference of red band and infrared band reflectivities and is used to monitor vegetation (Tucker, 1979). It is a numerical index that represents greenness of vegetation in an area. It is highly correlated with other vegetation parameters like leaf area index and canopy cover and thus serves as a good descriptor for vegetation discrimination (Gao et al., 2002). High values that are close to 1.0 represent temperate and tropical rainforests. From the observation of data it is seen that low positive values from 0.2 to 0.4 indicate the presence of shrubs and grasslands.

NDVI data is acquired from Earth Explorer website maintained by USGS. The 14-day NDVI composites are available for time period 1990 to 2008 at 7-day time step. There are 52 NDVI composites for each year obtained at a temporal resolution of 14 days with a 7-day moving time window. Some of the images with excessive noise produced by the clouds were removed from the analysis.

4.8.   Model Description

σ^o depends on vegetation characteristics, moisture content, and surface roughness of the land surface. This section describes an empirical model that relates water stage to $\sigma°$.

σ° is a function of several parameters given by equation 4.1.

$$\sigma^o = f\,(\lambda, \theta, p, \varepsilon, f, V)$$ Eqn. 4.1

where λ is wavelength, θ is incidence angle, p is polarization, ε is dielectric constant, f is surface roughness and V represents vegetation characteristics. The λ, θ, and p are radar observation parameters. Dielectric constant, surface roughness and vegetation type are land surface parameters that depend on water level, extent of corrugations on the surface and density of vegetation, respectively.
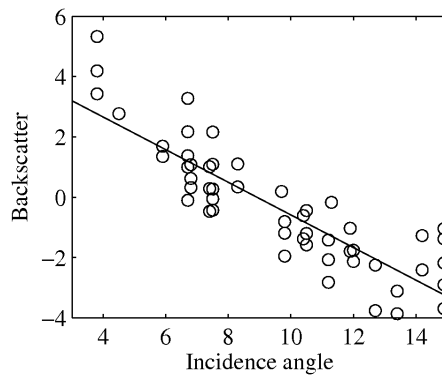
Figure 20 σ°-θ response at a site with low NDVI.

σ^o measurements are affected by incidence angle (θ) of observation. A typical σ° – θ plot for incidence angle range of 3 to 15 degrees is shown in Figure 20. The relative contribution from surface and vegetation scattering depends on the vegetation density and is reflected in the slope of σ°- θ response that for TRMMPR backscatter is approximated to be linear for angles between 3° and 15°. The σ°- θ is modeled as shown in equation 4.2.

71

$$\sigma°(\theta) = A + B \cdot (\theta - \theta_{ref})$$ Eqn. 4.2

where θ_{ref} is the reference angle, **A** (dB) is the backscatter normalized to θ_{ref} and **B** (dB/°) is the slope of the line fit. θ_{ref} is chosen to be 10°. In this research, multiple orbit $\sigma°$ measurements are used to prepare images of backscatter normalized to 10°.

A depends on the characteristics of the water surface. w_s is related to **A** as shown in equation 4.3.

$$w_s(A) = \mu_s + T \cdot A$$ Eqn. 4.3

where, w_s is water stage in ft. **μ_s** and **T** are the calibration parameters in (ft) and (ft/dB) respectively. **μ_s** denotes the modeled average value of water stage for the site under consideration. **T** is a weighing factor describing the linear relationship with normalized backscatter.

Figure 21 shows the backscatter from vegetation in bands– X (λ= 3 cm), C (λ= 6 cm), and L (λ= 25 cm). As the wavelength increases, the penetration of incident radiation into the vegetation increases and backscatter has greater contribution from the underlying surface. In case of water surface without any vegetation cover, the water's smooth surface results in specular reflection thus producing low backscatter. Backscatter increases with lowering of water level due to increase in the exposure of the vegetation above water.
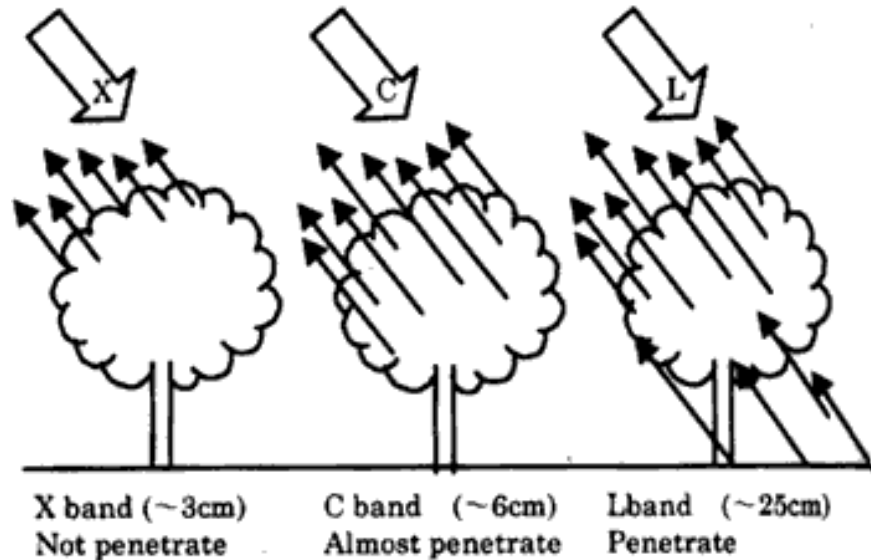
Figure 21 Backscatter from vegetation in bands X, C, and L (Iisaka et al., 1998).

The calibration of the model aims at obtaining the model parameters– μ_s and **T**. For every site, the w_s and **A** data are used to compute the model parameters by minimizing the error to obtain w_s from **A**. The model is calibrated using 75% of the time period to obtain model parameters μ_s and **T**. These model parameters are used to compute w_s for the remaining 25% of the data. The validation process comprises of comparing the w_s values obtained from the model with the observed w_s values. The correlation coefficient (R), root mean square error (rmse), and non-exceedance probability are computed between observed and modeled water stage and the accuracy of the model is assessed.

4.9.   Results and Discussions

The water stage model is applied over South Florida at 114 locations distributed

73

in 6 major landuse types i.e. woodland, wooded grassland, closed shrubland, open shrubland, grassland, and cropland. The model results for each landuse type are reported in this section. The model behavior over a representative site of the landuse is discussed with the help of time series plot of observed and modeled water stage. The scatterplot and non-exceedance probability plot of absolute error is also presented for a representative site of each landuse. This is followed by plots of scatterplot, non-exceedance probability plot, and boxplot distribution for combined data in each landuse type.

Figure 22 shows the results of the water stage model applied to woodland. Figure 22(a) shows the time series plot of observed and modeled water stage for 3 years of testing period. The highs and lows in water stage are caused by rainfall events or operation of control gates in the region. The model is able to capture the variation in water stage reasonably well. It follows the highs and lows in the water stage except for summer months when the model over-estimates the low values of water stage. Figure 22(b) shows the scatterplot of observed and modeled water stage with R=0.93 and root mean square error=0.70 ft. Over-estimation of stage is indicated by the data points lying above the 45° line and points falling below the line indicate under-estimation of the water stage. The over-estimation of water stage is evident in Figure 22(b). Figure 22(c) shows the non-exceedance probability on the horizontal axis and corresponding absolute error on the vertical axis. It can be seen from the figure that 59.7% of the water level, estimated by the model, have an error of 0.5 ft or less which increases to 85.8% for an

error of 1 ft or less. Woodland is characterized by tall vegetation (greater than 15 ft). The TRMMPR backscatter successfully captures the variation in exposed vegetation brought about by rise and fall of water stage in the area. In order to analyze the behavior of model in woodland, all the data from 22 woodland sites is combined in ensemble plots of scatterplot, non-exceedance probability, and boxplot distribution shown in Figure 22(d). All the points lie densely on the 45° line indicating a good performance of the model. The scatterplot gives a correlation of 0.99 and root mean square error of 0.65 ft indicating that the model works well over woodlands. According to the non-exceedance probability plot [see Figure 22(e)], 66.6% of data points have an error of 0.5 ft or less that increases to 91.0% of data points for an error of 1 ft or less. Figure 22(f) shows the distribution of observed and modeled water stage in the form of boxplot. The upper and lower edges of the box correspond to 75th and 25th percentile of the data. The horizontal line between the box is the median of the data set. The 95th percentile and 5th percentile are shown by whiskers above and below the box. The boxplot shows that the distributions of both observed and modeled water stage are quite similar.

According to Figure 22(a), the water stage ranges between 11 ft to 17 ft. The exposure of trees (> 15 ft) varies with the rise and fall of water stage. This partial submergence of trees affects the backscatter.

Figure 22 Water stage model as applied to wetlands in woodland. (a) time-series plot of observed and modeled water stage. (b) scatterplot of observed and modeled water stage (c) Non-exceedance probability plot (d) combined scatterplot of observed and modeled water stage for all the woodland sites (e) combined non-exceedance probability plot (f) boxplot distribution of observed and modeled water stage.

The results for water stage model over wooded grassland are shown in Figure 23. Wooded grassland is characterized with tree canopy cover between 10% and 40% and tree heights greater than 15 ft. The model captures the variation in water stage with correlation coefficient =0.89 and root mean square error= 0.47 ft [Figure 23 (a-c)]. The non-exceedance probability plot reveals that 99.3% of the estimates have an absolute error of 1 ft or less. This indicates that the model performs well. During the period when the water inundation is high, most of the vegetation gets submerged under water rendering the surface as smooth that result in low backscatter. High correlation between observed and modeled water stage obtained at this site shows the applicability of model over wooded grassland. Furthermore, the applicability of the model is also assessed for

the combined group behavior of 20 sites in wooded grassland. Most of the data points lie along the 45° line with correlation=0.98 and root mean square error=0.65 as shown in Figure 23(d). The non-exceedance probability plot in Figure 23(e) shows that 73.2% of the water level estimates have an absolute error of 0.5 ft or less and 93.7% of the water level estimates have an absolute error of 1 ft or less. The boxplot representing 25th percentile and 75th percentile match with each other well. Thus, the model results for woodland in Figure 22 and wooded grassland in Figure 23 produce similar results as both the landuse categories consist of tall vegetation with trees greater than 15 ft. The seasonal rise and fall of water stage is also captured reasonably well.

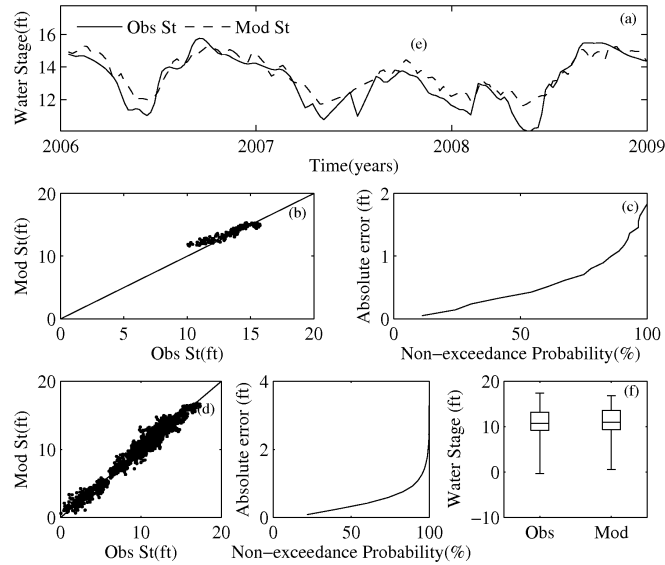Figure 23 Water stage model as applied to wetlands in wooded grassland. (a) time-series plot of observed and modeled water stage. (b) scatterplot of observed and modeled water stage (c) Non-exceedance probability plot (d) combined scatterplot of observed and modeled water stage for all the wooded grassland sites (e) combined non-exceedance probability plot (f) boxplot distribution of observed and modeled water stage.

Similar model results for sites in closed shrubland are shown in Figure 24. Closed shrubland surface is dominated by shrubs that are less than 15 ft in height. The modeled water stage for 2 years of testing data compares well with observed water stage. The model works well for the representative site capturing the highs and lows of the water stage variation with R=0.86 and root mean square error=0.51 ft. The non-exceedance plot [Figure 24(c)] shows that 66.9% of the water levels, estimated by the model at this site have an absolute error of 0.5 ft and 95.4% of the estimates have an absolute error of 1 ft or less.

In the scatterplot, the points lie along the 45° line with R=0.99 and root mean square error=0.53 ft; whereas in the non-exceedance probability plot, 72.1% of the data points have an error of 0.5 ft or less and 94.3% of the data points have an error of 1 ft or less. The boxplot shows that the 25th percentile, median, and 75th percentile of modeled water stage match well with that of observed water stage. In closed shrubland though the tree heights are less than 15 ft, the canopy cover of bushes and shrubs is greater than 40% and is spread across the water stage in the region. Thus the behavior of closed shrubland resembles that of woodland and wooded grassland. This is because of the variation in water stage that causes partial submergence of bushes and shrubs affecting the backscatter measurements.
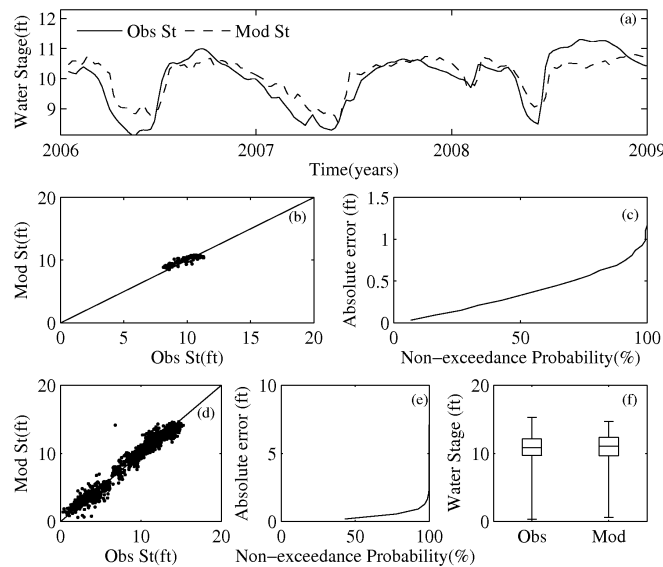
Figure 24 Water stage model as applied to wetlands in closed shrubland. (a) time-series plot of observed and modeled water stage. (b) scatterplot of observed and modeled water stage (c) Non-exceedance probability plot (d) combined scatterplot of observed and modeled water stage for all the closed shrubland sites (e) combined non-exceedance probability plot (f) boxplot distribution of observed and modeled water stage.

The model result as applied to open shrubland is shown in Figure 25. Unlike closed shrubland, open shrubland consists of tree with height less than 6 ft and less canopy cover. The result for 2 years of testing data of the model applied to a representative site of open shrubland is shown in Figure 25(a-c). The model is unable to capture high water stages observed in the end of year 2008. The scatterplot for the site depicts R=0.84 and root mean square error=0.42. The non-exceedance probability plot shows that 84.9% of the estimates have an error of 0.5 ft or less and 96.8% of the estimates have an error of 1 ft or less.

The scatterplot of the data points of all 17 open shrubland sites show three clusters ranging from low water stage, medium water stage to high water stage. It is

79

seen from the figure that the model works well for all the water stages giving a combined R=0.99 and root mean square error of 0.57 ft. The non-exceedance probability plot shows that 70.0% of the water levels, estimated by the model have an error of 0.5 ft or less and 93.2% of the estimates have an error of 1 ft or less. The boxplot distribution shows the model works well to identify most of the range of data points except for high stages represented by 95th whisker and low water stage represented by 5th percentile. Most of the vegetation in open shrubland (< 6 ft) remains submerged under water for most part of the year.

Figure 25 Water stage model as applied to wetlands in open shrubland. (a) time-series plot of observed and modeled water stage. (b) scatterplot of observed and modeled water stage (c) Non-exceedance probability plot (d) combined scatterplot of observed and modeled water stage for all the open shrubland sites (e) combined non-exceedance probability plot (f) boxplot distribution of observed and modeled water stage.

The performance of the model in the area of grassland is shown in Figure 26.

80

Grassland is covered with continuous herbaceous cover consisting of less than 10% tree canopy cover. The model works well and has captured the variation in water stage well [Figure 26(a-c)]. The representative site for grassland lies in Everglades and shows the efficiency of applicability of the model for the grassland as the data points lie near the 45° line indicating good model performance. Model performance for this site is high since correlation is 0.85 and root mean square error is 0.52 ft. The non-exceedance probability plot shows that 77.3% of the data has 0.5 ft or less error in the estimates which increases to 1.0 ft or less error for 92.1% of the estimates.

The combined result of applicability of model to all 36 grassland sites is summarized in Figure 26(d-f). The model works reasonably well since the scatterplot gives a high correlation of 0.98 and root mean square error of 0.66 ft. The non-exceedance probability plot for grassland shows that 92.1% of the water stage estimates have an error of 1 ft or less. The water in grassland is spread over the herbaceous cover. Lowering of water stage in grassland exposes the herbaceous cover and most of the backscatter obtained by the TRMMPR is from the vegetated surface. On the other hand, high stage values submerge the herbaceous cover of vegetation and render the surface as smooth which decreases the amount of backscatter as most of the incident radiation is specularly reflected from the water surface.
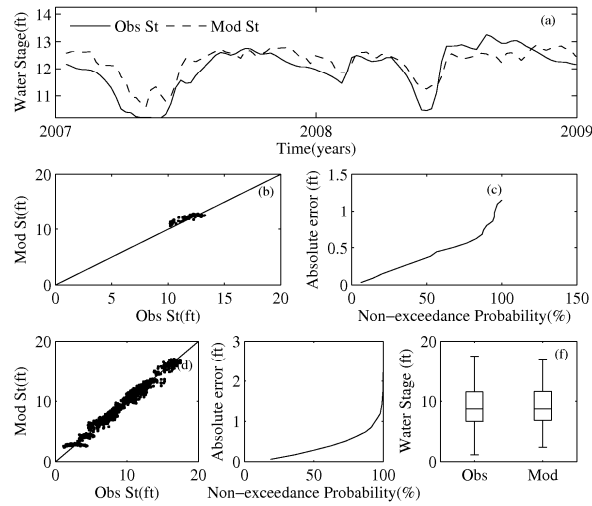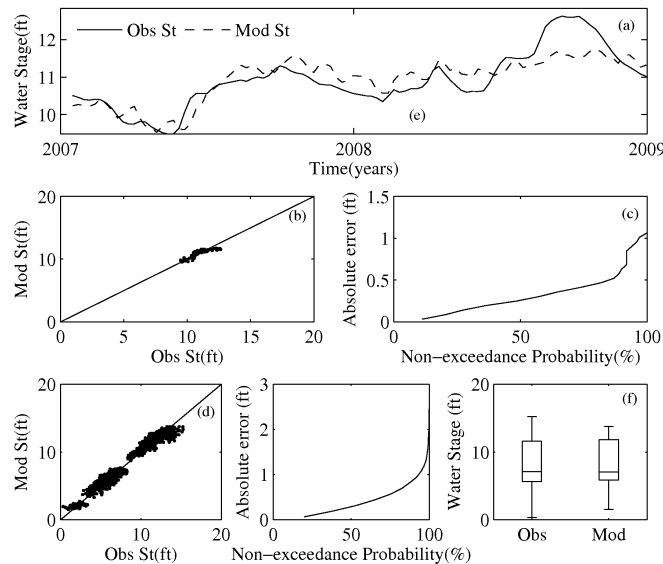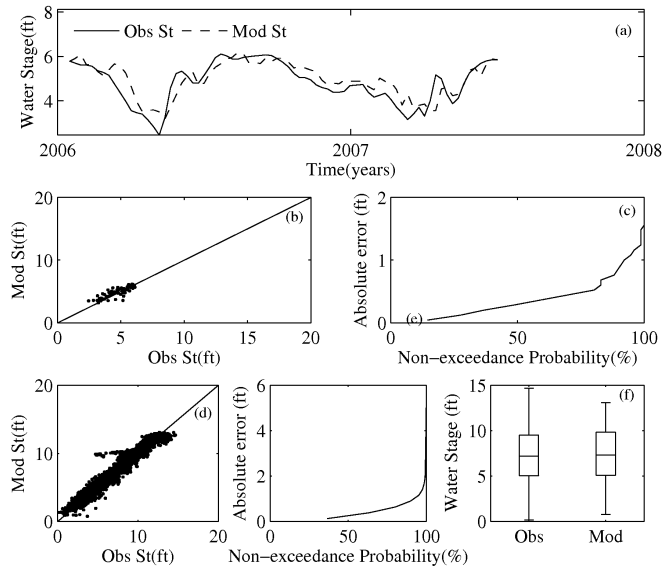
Figure 26 Water stage model as applied to wetlands in grassland. (a) time-series plot of observed and modeled water stage. (b) scatterplot of observed and modeled water stage (c) Non-exceedance probability plot (d) combined scatterplot of observed and modeled water stage for all the grassland sites (e) combined non-exceedance probability plot (f) boxplot distribution of observed and modeled water stage.

The behavior of model for cropland is shown in Figure 27. The model works well at this site with R=0.79 and root mean square error=0.59 ft. The non-exceedance probability plot shows that 60.0% of the water level estimates have an error of 0.5 ft or less and 92.2% of the estimates have an error of 1 ft or less [Figure 27(a-c)].

The model result for a combined analysis of all the 4 cropland sites shows the scatterplot of observed and modeled soil moisture. The majority of the points are located along the 45° line with R=0.91 and root mean square error=0.60 ft. The probabilistic absolute error curve shows that 67.3% of the estimates have an error of 0.5 ft or less which increases to 1 ft or less error for 91.9% of the estimates. The modeled water stage captures the behavior of observed water stage well. The stage values in cropland ranges

from 1 ft to 6 ft. This keeps the vegetation under partial submergence the affect of which is captured in the backscatter.
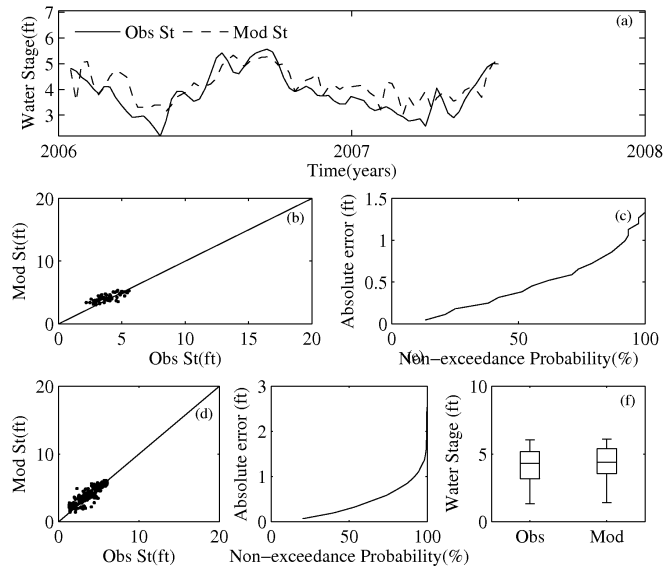
Figure 27 Water stage model as applied to wetlands in cropland. (a) time-series plot of observed and modeled water stage. (b) scatterplot of observed and modeled water stage (c) Non-exceedance probability plot (d) combined scatterplot of observed and modeled water stage for all the cropland sites (e) combined non-exceedance probability plot (f) boxplot distribution of observed and modeled water stage.

A summary of model performance for all the landuse categories described above is listed in Table 4. All landuses have a high correlation value (0.98-0.99) except for cropland which has 0.91. This is because of fewer number of sites in this landuse (=4) whereas the number of sites in other landuse types is 15 or more. It can also be observed from the table that with the exception to cropland, the landuse with greater number of sites gives higher root mean square error as compared to landuse that has lesser number of sites. The range of root mean square error is between 0.53 ft and 0.66 ft. This shows

83

that the model works well for every landuse type. This is also confirmed by the percentage of sites that give an error of 1 ft or less as all the landuse type has more than 91% of data points that give an error of 1 ft or less.

Table 4 Model performance in various landuse types.

Landuse	Number of sites	R	rmse (ft)	Percentage of estimates with error < 5%	Percentage of estimates with error < 10%
Grassland	36	0.98	0.66	71.1%	92.1%
Woodland	22	0.99	0.65	66.6%	91.0%
Wooded Grassland	20	0.98	0.65	73.2%	93.7%
Cropland	4	0.91	0.60	67.3%	91.9%
Open Shrubland	17	0.99	0.57	70.0%	93.2%
Closed Shrubalnd	15	0.99	0.53	72.1%	94.3%

Figure 28 shows the combined model results as applied to all the water stage sites in the study area. A good match between observed and modeled water stage is observed with high correlation of 0.99 and root mean square error of 0.63 ft in the scatterplot [Figure 28(a)]. Figure 28(b) shows that 74.7% of estimates have an absolute error of 0.5 ft or less which increases to 93.5% of estimates having error of 1 ft or less. The boxplot distribution in Figure 28(c) shows that the distribution of modeled water stage is well representing the distribution of observed water stage except for very low water stage values close to zero. This suggests that the water stage model works reasonably well for all the sites in wetland region of South Florida.
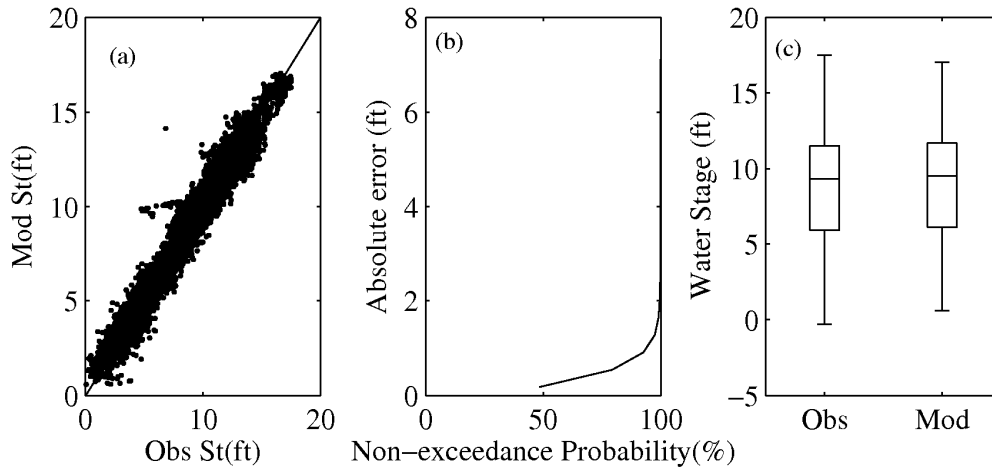
Figure 28 Water stage model as applied to all the water stage sites in wetlands of South Florida. (a) combined scatterplot of observed and modeled water stage for all the sites (b) combined non-exceedance probability plot (c) boxplot distribution of observed and modeled water stage.

Results show that the model that relates w_s to $\sigma°$ works reasonably well for all landuses in the study area. In order to obtain better understanding of the role of vegetation in the proposed model, NDVI is added into the model, as shown in equation 4.4.

$$w_s(A, NDVI) = \mu_s + \mathbf{T} \cdot A + \mathbf{P} \cdot (NDVI - \mu_{ndvi}) \qquad \text{Eqn. (4.4)}$$

where, $\mathbf{P}$ is the weighing factor describing the effect of NDVI and μ_{ndvi} is the average NDVI over the calibration period.

The model calibration parameters and model assessment parameters for two cases i.e., with and without NDVI in the model for representative sites of each landuse are compared in Table 5. Model calibration and assessment parameters are similar for both the cases for most landuse types except for grassland and cropland. This is because grassland and cropland do not have any tall vegetation and consists of herbaceous cover

85

and crop producing fields, respectively. NDVI is an index that measures the greenness of vegetation. The greenness is strongly linked to geometry in case of grassland and cropland but has a weak link with geometry in case of woodland, wooded grassland, and shrubland. In woodland, wooded grassland, and shrubland, the vegetation remains same for the whole year. However, in case of cropland, the physical changes are brought about by the crop cycle of seeding and harvesting which changes the geometrical characteristics of the cropland. Similarly, there is a greater variation in greenness of grassland throughout the year as compared to other landuse types. Hence, it is seen that NDVI impacts the results for grassland and cropland but not for other landuse types.

Table 5 Model parameters and results for various landuse type.

Landuse	Without NDVI				With NDVI				
	μ_s	T	R	rmse	μ_s	T	P	R	rmse
Woodland	15.54	0.45	0.93	0.70	15.54	0.45	-0.25	0.94	0.70
Cropland	5.97	0.45	0.79	0.59	5.97	0.45	-1.29	0.81	0.59
Closed Shrubland	12.93	0.28	0.86	0.51	12.92	0.28	-1.18	0.86	0.51
Grassland	6.22	0.42	0.85	0.52	6.24	0.42	-1.74	0.86	0.52
Wooded Grassland	10.84	0.23	0.89	0.47	10.84	0.23	0.13	0.89	0.47
Open Shrubland	11.42	0.26	0.84	0.42	11.43	0.26	-0.17	0.84	0.42

4.10. Conclusions

A simple empirical model is developed that relates water stage to TRMMPR backscatter measurements. Backscatter depends on the dielectric and physical characteristics of the target area. The backscatter dependence on the partial submergence

86

of vegetation is used as the basis of estimation of water stage from backscatter measurements.

A simple linear model relating backscatter and stage is developed that works reasonably well over various landuse types in South Florida. For various landuse types, the combined correlation between observed and modeled water stage is 0.99 and root mean square error is 0.63 ft. A high correlation and low root mean square error shows the strength of the model. Individual landuse types also show high correlation (0.98-0.99) and low root mean square error (0.53 ft – 0.66 ft) between observed and modeled water stage.

A model relating water stage to TRMMPR backscatter and NDVI is also developed and tested. NDVI accounting for vegetation density increases the model performance for grassland and cropland. This is because greenness of vegetation measured by NDVI has a strong link with the geometrical characteristics of the grassland and cropland. On the other landuse types that are characterized by tall trees and shrubs– woodland, wooded grassland, open shrubland, and closed shrubland, NDVI in the model does not improve the results. This is because there is not much variation in the vegetation growth from one season to the other as seen in grassland and cropland brought about by the crop cycle and seasons of seeding and harvesting of crops.

This research provides an alternative method of estimating water stage using spaceborne backscatter measurements. Moreover, this research gives an insight into the effect of water level in partially inundated vegetation on the radar backscatter. This can

87

help scientists, engineers, and policy-makers to understand the comprehensive spatial and temporal variability of water stage without installing many measuring gages.

4.11. References

Brande, J. (1980). Worthless, Valuable, or What - an Appraisal of Wetlands. Journal of Soil and Water Conservation, 35(1), 12-16.

Covich, A. P., Fritz, S. C., Lamb, P. J., Marzolf, R. D., Matthews, W. J., Poiani, K. A., et al. (1997). Potential effects of climate change on aquatic ecosystems of the Great Plains of North America. Hydrological Processes, 11(8), 993-1021.

Daily, G. C. (1997). Nature's services: Societal dependence on natural ecosystems. Washington, D.C., USA: Island Press.

Doren, R. F., Rutchey, K., & Welch, R. (1999). The Everglades: A perspective on the requirements and applications for vegetation map and database products. Photogrammetric Engineering and Remote Sensing, 65(2), 155-161.

Fennema, R. J., Neidrauer, C. J., Johnson, R. A., MacVicar, T. K., & Perkins, W. A. (1994). A computer model to simulate natural south Florida hydrology. Florida, USA: St. Lucie Press.

Gao, F., Jin, Y. F., Li, X. W., Schaaf, C. B., & Strahler, A. H. (2002). Bidirectional NDVI and atmospherically resistant BRDF inversion for vegetation canopy. Ieee Transactions on Geoscience and Remote Sensing, 40(6), 1269-1278.

Gorham, E., Dean, W. E., & Sanger, J. E. (1983). The Chemical-Composition of Lakes in the North-Central United-States. Limnology and Oceanography, 28(2), 287-301.

Gotkiewicz, J. (2005). Paludology as a science of wetlands. Advances of Agricultural Sciences Problems Issues, (507), 159-164

Isaka, J. (1998). Synthetic aperture radar image handbook. Asakura, Tokyo.

Johnson, W. C., Boettcher, S. E., Poiani, K. A., & Guntenspergen, G. (2004). Influence of weather extremes on the water levels of glaciated prairie wetlands. Wetlands, 24(2), 385-398.

Kummerow, C., Barnes, W., Kozu, T., Shiue, J., & Simpson, J. (1998). The Tropical Rainfall Measuring Mission (TRMM) sensor package. Journal of Atmospheric and Oceanic Technology, 15(3), 809-817.

Kushlan, J. A. (1990). Wetlands and Wildlife, the Everglades Perspective in Freshwater Wetlands and Wildlife. Tennessee, USA: Department of Energy.

McAllister, L. S., Peniston, B. E., Leibowitz, S. G., Abbruzzese, B., & Hyman, J. B. (2000). A synoptic assessment for prioritizing wetland restoration efforts to optimize flood attenuation. Wetlands, 20(1), 70-83.

Ozesmi, S. L., & Bauer, M. E. (2002). Satellite remote sensing of wetlands. [10.1023/A:1020908432489]. Wetlands Ecology and Management, 10(5), 381-402.

Pant, H. K., Rechcigl, J. E., & Adjei, M. B. (2003). Carbon sequestration in wetlands: concept and estimation. ournal of Food, Agriculture & Environment, 1(2), 308-313.

Tucker, C. J. (1979). Red and Photographic Infrared Linear Combinations for Monitoring Vegetation. Remote Sensing of Environment, 8(2), 127-150.

Wdowinski, S., Kim, S. W., Amelung, F., Dixon, T. H., Miralles-Wilhelm, F., & Sonenshein, R. (2008). Space-based detection of wetlands' surface water level changes from L-band SAR interferometry. Remote Sensing of Environment, 112(3), 681-696.

Zhang, B. (2008). Data Mining, GIS and Remote Sensing: Application in wetland hydrological investigation., Ohio State University, Ohio.

CHAPTER 5

CONCLUSIONS AND RECOMMENDATIONS

This study presents the applications of microwave remote sensing in measuring the soil moisture and water stage from space. In this thesis, models are developed that relate soil moisture and water stage to backscatter measurements. This chapter summarizes the goals and important results of this research. The conclusions identify new research ideas that are listed as recommendations. The limitations and applications of this research are also described.

To address the first research question in this research, soil moisture is relate to $\sigma°$ and NDVI. $\sigma°$ being sensitive to dielectric properties is able to capture the soil moisture in the target area efficiently. The impact of landuse type on each site is also taken into consideration. The estimated values from the model are compared to the observed values and the performance of the model is assessed.

To address the second research question in this research, water stage in wetlands of South Florida is related to $\sigma°$. The dependence of $\sigma°$ on the partial submergence of vegetation is used as the basis for the study. The effect of vegetation on the model is assessed by comparing two model cases– (a) that does not include NDVI, and (b) that includes NDVI in the model.

5.1. Conclusions

Microwave remote sensing has proved to be a useful tool in measurement of soil

moisture from the space in the past. In the past research, most of such research work has been conducted using passive microwave remote sensing. This research uses active microwave remote sensing to relate soil moisture and water stage to backscatter measurements from TRMMPR. The key results of this research are listed below.

1. TRMMPR backscatter is related to soil moisture. Within the incidence angle range of 3 to 15 degrees, there is a linear relationship between σ° and soil moisture.

2. The relationship of σ° and soil moisture is dependent on the vegetation density. Soil moisture estimation improves with incorporation of NDVI into the model.

3. σ° is affected by changes in the water stage. This relation is explained through the changes in the physical characteristics from varying submergence of vegetation in the inundated areas.

4. Taking into effects of NDVI while estimating water stage in wetlands improves the results for grasslands and croplands.

5.2. Recommendations

Based on the above conclusions, few limitations, new questions and research ideas are also identified. These could be investigated to extend the research work presented in this thesis. Suggestions to address those limitations and extend this work include the following.

1. The spatial resolution used for developing soil moisture model is default 4.4 km resolution of TRMMPR backscatter. The spatial resolution of water stage model is

91

arbitrarily selected to be 2 km. An optimal spatial resolution with less noise and high resolution could be selected for the research.

2. The analysis of TRMMPR backscatter variation with incidence angle could be done for water stage model to find the optimum incidence angle that could give better results.

3. LAI is a better measure of vegetation density in terms of the surface area of the leaves as compared to NDVI. Hence, LAI could be used in place of NDVI in future work.

4. The surface roughness could be calculated and its effects could be incorporated in the model.

5. The soil moisture and water stage models could be tested at other locations with different sources of data.

6. The temporal averaging could be done for seven days to obtain behavior at a higher temporal resolution.

5.3.   Limitations

Some of the limitations of the soil moisture and water stage models are listed below.

Soil Moisture

1. Radar backscatter is also sensitive to soil surface roughness. This research relates backscatter to soil moisture and vegetation without considering the effects of surface roughness.

2. Backscatter is related to soil moisture and vegetation using a linear model which

92

provides reasonable estimates over arid regions of Southern US. The model performance would deteriorate over mountainous terrains.

3. Ku band waves are scattered by leaves that are comparable to wavelength 2.2 cm. Due to this attenuation, the model doesn't perform well in dense vegetation.

4. The model requires ground data for calibration that is point specific.

Water Stage

1. Model performance deteriorates with reduction in vegetation density over the free water.

2. In case of mostly or completely inundated vegetation, the specular reflection dominates and model would not work.

3. The model requires ground data for calibration.

The research explains the backscatter dependence on the soil moisture and water stage. The effect of vegetation cover and landuse is also considered.

1. The calibrated models can be used to estimate soil moisture and water stage at selected sites using the TRMMPR and NDVI data in future.

2. The understanding developed in this research leads to development of spatial maps of soil moisture and water stage.

This research explores active microwave remote sensing for the estimation of soil moisture and water stage from space. Soil moisture and water stage models developed in this research provide a novel way of measuring soil moisture and water stage.

REFERENCES

Alsdorf, D. E., Melack, J. M., Dunne, T., Mertes, L. A. K., Hess, L. L., & Smith, L. C. (2000). Interferometric radar measurements of water level changes on the Amazon flood plain. Nature, 404(6774), 174-177.

Barrett, B., Dwyer, E., & Whelan, P. (2009). Soil Moisture Retrieval from Active Spaceborne Microwave Observations: An Evaluation of Current Techniques. Remote Sensing, 1(3), 210-242.

Bourgeau-Chavez, L. L., Smith, K. B., Brunzell, S. M., Kasischke, E. S., Romanowicz, E. A., & Richardson, C. J. (2005). Remote monitoring of regional inundation patterns and hydroperiod in the greater everglades using synthetic aperture radar. Wetlands, 25(1), 176-191.

Covich, A. P., Fritz, S. C., Lamb, P. J., Marzolf, R. D., Matthews, W. J., Poiani, K. A., et al. (1997). Potential effects of climate change on aquatic ecosystems of the Great Plains of North America. Hydrological Processes, 11(8), 993-1021.

Crosson, W. L., Laymon, C. A., Inguva, R., & Schamschula, M. P. (2002). Assimilating remote sensing data in a surface flux-soil moisture model. Hydrological Processes, 16(8), 1645-1662.

Daily, G. C. (1997). Nature's services: Societal dependence on natural ecosystems. Washington, D.C., USA: Island Press.

Das, N. N., Mohanty, B. P., Cosh, M. H., & Jackson, T. J. (2008). Modeling and assimilation of root zone soil moisture using remote sensing observations in Walnut Gulch Watershed during SMEX04. Remote Sensing of Environment, 112(2), 415-429.

Dobson, M. C., & Ulaby, F. (1981). Microwave Backscatter Dependence on Surface-Roughness, Soil-Moisture, and Soil Texture .3. Soil Tension. Ieee Transactions on Geoscience and Remote Sensing, 19(1), 51-61.

Dobson, M. C., & Ulaby, F. T. (1986). Active Microwave Soil-Moisture Research. Ieee Transactions on Geoscience and Remote Sensing, 24(1), 23-36.

Du, Y., Ulaby, F. T., & Dobson, M. C. (2000). Sensitivity to soil moisture by active and passive microwave sensors. Ieee Transactions on Geoscience and Remote Sensing, 38(1), 105-114.

Engman, E. T., & Chauhan, N. (1995). Status of Microwave Soil-Moisture Measurements with Remote-Sensing. Remote Sensing of Environment, 51(1), 189-198.

Ferraro, R. R. (1997). Special sensor microwave imager derived global rainfall estimates for climatological applications. Journal of Geophysical Research-Atmospheres, 102(D14), 16715-16735.

Frappart, F., Seyler, F., Martinez, J.-M., León, J. G., & Cazenave, A. (2005). Floodplain water storage in the Negro River basin estimated from microwave remote sensing of inundation area and water levels. [doi: DOI: 10.1016/j.rse.2005.08.016]. Remote Sensing of Environment, 99(4), 387-399.

Gao, H., Wood, E. F., Jackson, T. J., Drusch, M., & Bindlish, R. (2006). Using TRMM/TMI to retrieve surface soil moisture over the southern United States from 1998 to 2002. Journal of Hydrometeorology, 7(1), 23-38.

Gorham, E., Dean, W. E., & Sanger, J. E. (1983). The Chemical-Composition of Lakes in the North-Central United-States. Limnology and Oceanography, 28(2), 287-301.

Hansen, M. C., Defries, R. S., Townshend, J. R. G., & Sohlberg, R. (2000). Global land cover classification at 1km spatial resolution using a classification tree approach. International Journal of Remote Sensing, 21(6-7), 1331-1364.

Hess, L. L., Melack, J. M., Filoso, S., & Yong, W. (1995). Delineation of inundated area and vegetation along the Amazon floodplain with the SIR-C synthetic aperture radar. Geoscience and Remote Sensing, IEEE Transactions on, 33(4), 896-904.

Hess, L. L., Melack, J. M., & Simonett, D. S. (1990). Radar detection of flooding beneath the forest canopy - a review. International Journal of Remote Sensing, 11, 1313-1325.

Jackson, T. J. (1993). Measuring Surface Soil-Moisture Using Passive Microwave Remote-Sensing .3. Hydrological Processes, 7(2), 139-152.

Jackson, T. J., Bindlish, R., Gasiewski, A. J., Stankov, B., Klein, M., Njoku, E. G., et al. (2005). Polarimetric scanning radiometer C- and X-band microwave observations during SMEX03. Ieee Transactions on Geoscience and Remote Sensing, 43(11), 2418-2430.

Jackson, T. J., Chang, A., & Schmugge, T. J. (1981). Aircraft Active Microwave Measurements for Estimating Soil-Moisture. Photogrammetric Engineering and Remote Sensing, 47(6), 801-805.

Jackson, T. J., Levine, D. M., Swift, C. T., Schmugge, T. J., & Schiebe, F. R. (1995). Large-Area Mapping of Soil-Moisture Using the Estar Passive Microwave Radiometer in Washita92. Remote Sensing of Environment, 54(1), 27-37.

Johnson, W. C., Boettcher, S. E., Poiani, K. A., & Guntenspergen, G. (2004). Influence of weather extremes on the water levels of glaciated prairie wetlands. Wetlands, 24(2), 385-398.

Kasischke, E. S., Smith, K. B., Bourgeau-Chavez, L. L., Romanowicz, E. A., Brunzell, S., & Richardson, C. J. (2003). Effects of seasonal hydrologic patterns in south Florida wetlands on radar backscatter measured from ERS-2 SAR imagery. Remote Sensing of Environment, 88(4), 423-441.

Kozu, T., Kawanishi, T., Kuroiwa, H., Kojima, M., Oikawa, K., Kumagai, H., et al. (2001). Development of precipitation radar onboard the Tropical Rainfall Measuring Mission (TRMM) satellite. Ieee Transactions on Geoscience and Remote Sensing, 39(1), 102-116.

Kummerow, C., Simpson, J., Thiele, O., Barnes, W., Chang, A. T. C., Stocker, E., et al. (2000). The status of the Tropical Rainfall Measuring Mission (TRMM) after two years in orbit. Journal of Applied Meteorology, 39(12), 1965-1982.

LaBaugh, J. W., Winter, T. C., Swanson, G. A., Rosenberry, D. O., Nelson, R. D., & Euliss, N. H. (1996). Changes in atmospheric circulation patterns affect midcontinent wetlands sensitive to climate. Limnology and Oceanography, 41(5), 864-870.

Larson, K. M., Small, E. E., Gutmann, E., Bilich, A., Axelrad, P., & Braun, J. (2008). Using GPS multipath to measure soil moisture fluctuations: initial results. Gps Solutions, 12(3), 173-177.

Martin, D. B., & Hartman, W. A. (1987). The Effect of Cultivation on Sediment Composition and Deposition in Prairie Pothole Wetlands. Water Air and Soil Pollution, 34(1), 45-53.

Mertes, L. A. K., Daniel, D. L., Melack, J. M., Nelson, B., Martinelli, L. A., & Forsberg, B. R. (1995). Spatial patterns of hydrology, geomorphology, and vegetation on the floodplain of the Amazon river in Brazil from a remote sensing perspective. [doi: DOI: 10.1016/0169-555X(95)00038-7]. Geomorphology, 13(1-4), 215-232.

Moran, M. S., Peters-Lidard, C. D., Watts, J. M., & McElroy, S. (2004). Estimating soil moisture at the watershed scale with satellite-based radar and land surface models. Canadian Journal of Remote Sensing, 30(5), 805-826.

Mulhouse, J. M., & Galatowitsch, S. M. (2003). Revegetation of prairie pothole wetlands in the mid-continental US: twelve years post-reflooding. Plant Ecology, 169(1), 143-159.

Njoku, E. G., & Entekhabi, D. (1996). Passive microwave remote sensing of soil moisture. Journal of Hydrology, 184(1-2), 101-129.

Njoku, E. G., Jackson, T. J., Lakshmi, V., Chan, T. K., & Nghiem, S. V. (2003). Soil moisture retrieval from AMSR-E. Ieee Transactions on Geoscience and Remote Sensing, 41(2), 215-229.

Oki, T., Seto, S., & Musiake, K. (2000). Land surface monitoring by backscattering coefficient from TRMM/PR 2A21. Paper presented at the Geoscience and Remote Sensing Symposium, 2000. Proceedings. IGARSS 2000. IEEE 2000 International.

Ozesmi, S. L., & Bauer, M. E. (2002). Satellite remote sensing of wetlands. [10.1023/A:1020908432489]. Wetlands Ecology and Management, 10(5), 381-402.

Paloscia, S., Macelloni, G., Santi, E., & Koike, T. (2001). A multifrequency algorithm for the retrieval of soil moisture on a large scale using microwave data from SMMR and SSM/I satellites. Ieee Transactions on Geoscience and Remote Sensing, 39(8), 1655-1661.

Pauwels, V. R. N., Timmermans, W., & Loew, A. (2008). Comparison of the estimated water and energy budgets of a large winter wheat field during AgriSAR 2006 by multiple sensors and models. Journal of Hydrology, 349(3-4), 425-440.

Piechota, T., Timilsena, J., Tootle, G., & Hidalgo, H. (2004). The western US drought: How bad is it. EOS, 85(32), 301-304

Pope, K. O., Reybenayas, J. M., & Paris, J. F. (1994). Radar remote sensing of forest and wetland ecosystem in the central-american tropics. Remote Sensing of Environment, 48(2), 205-219.

Richards, J. A., Woodgate, P. W., & Skidmore, A. K. (1987). An explanation of enhanced radar backscattering from flooded forests. International Journal of Remote Sensing, 8(7), 1093-1100.

Schneider, K., Huisman, J. A., Breuer, L., Zhao, Y., & Frede, H. G. (2008). Temporal stability of soil moisture in various semi-arid steppe ecosystems and its application in remote sensing. Journal of Hydrology, 359(1-2), 16-29.

Sippe, S. J., Hamilton, S. K., Melack, J. M., & Novo, E. M. M. (1998). Passive microwave observations of inundation area and the area/stage relation in the Amazon River floodplain. International Journal of Remote Sensing, 19(16), 3055 - 3074.

Song, D. S., Zhao, K., & Guan, Z. (2007). Advances in research on soil moisture by microwave remote sensing in China. Chinese Geographical Science, 17(2), 186-191.

Su, Z. B., Yacob, A., Wen, J., Roerink, G., He, Y. B., Gao, B. H., et al. (2003). Assessing relative soil moisture with remote sensing data: theory, experimental validation, and application to drought monitoring over the North China Plain. Physics and Chemistry of the Earth, 28(1-3), 89-101.

Swanson, G. A. (1988). Aquatic habitats of breeding waterfowl (Vol. 1). Portland, USA: Timber Press.

Swanson, G. A., & Duebbert, H. F. (1989). Wetland habitats of waterfowl in the Prairie Pothole Region. Iowa, USA: University Press.

Ulaby, F. T., & Batlivala, P. P. (1976). Optimum Radar Parameters for Mapping Soil-Moisture. Ieee Transactions on Geoscience and Remote Sensing, 14(2), 81-93.

Ulaby, F. T., Batlivala, P. P., & Dobson, M. C. (1978). Microwave Backscatter Dependence on Surface-Roughness, Soil-Moisture, and Soil Texture .1. Bare Soil. Ieee Transactions on Geoscience and Remote Sensing, 16(4), 286-295.

Ulaby, F. T., Dobson, M. C., & Bradley, G. A. (1981). Radar reflectivity of bare and vegetation-covered soil. [doi: DOI: 10.1016/0273-1177(81)90384-7]. Advances in Space Research, 1(10), 91-104.

Ulaby, F. T., Moore, R. K., & Fung, A. K. (1986). Microwave remote sensing: Active and passive. (Vol. 3). Massachusetts, USA: Artech House, Inc.

Valk, A. G. v. d. (2005). Water-level fluctuations in North American prairie wetlands. [10.1007/s10750-004-4866-3]. Hydrobiologia, 539(1), 171-188.

van Zyl, J. J., Njoku, E. G., & Jackson, T. J. (2003). Quantitative analysis of SMEX'02 AIRSAR data for soil moisture inversion. Paper presented at the Geoscience and Remote Sensing Symposium, 2003. IGARSS '03. Proceedings. 2003 IEEE International.

Verhoest, N. E. C., Troch, P. A., Paniconi, C., & De Troch, F. P. (1998). Mapping Basin Scale Variable Source Areas From Multitemporal Remotely Sensed Observations of Soil Moisture Behavior. Water Resour. Res., 34.

Vivoni, E. R., Gebremichael, M., Watts, C. J., Bindlish, R., & Jackson, T. J. (2008). Comparison of ground-based and remotely-sensed surface soil moisture estimates over complex terrain during SMEX04. Remote Sensing of Environment, 112(2), 314-325.

Wagner, W., Lemoine, G., & Rott, H. (1999). A method for estimating soil moisture from ERS scatterometer and soil data. Remote Sensing of Environment, 70(2), 191-207.

Wagner, W., Scipal, K., Pathe, C., Gerten, D., Lucht, W., & Rudolf, B. (2003). Evaluation of the agreement between the first global remotely sensed soil moisture data with model and precipitation data. Journal of Geophysical Research-Atmospheres, 108(D19), -.

Wang, J. R., Engman, E. T., Shiue, J. C., Rusek, M., & Steinmeier, C. (1986). The Sir-B Observations of Microwave Backscatter Dependence on Soil-Moisture, Surface-Roughness, and Vegetation Covers. Ieee Transactions on Geoscience and Remote Sensing, 24(4), 510-516.

Wang, J. R., Hsu, A., Shi, J. C., ONeill, P. E., & Engman, E. T. (1997). A comparison of soil moisture retrieval models using SIR-C measurements over the Little Washita River watershed. Remote Sensing of Environment, 59(2), 308-320.

Wang, Y., Hess, L. L., Filoso, S., & Melack, J. M. (1995). Understanding the radar backscattering from flooded and nonflooded Amazonian forests: Results from canopy backscatter modeling. [doi: DOI: 10.1016/0034-4257(95)00140-9]. Remote Sensing of Environment, 54(3), 324-332.

Wdowinski, S., Amelung, F., Miralles-Wilhelm, F., Dixon, T. H., & Carande, R. (2004). Space-based measurements of sheet-flow characteristics in the Everglades wetland, Florida. Geophysical Research Letters, 31(15), -.

Wdowinski, S., Kim, S. W., Amelung, F., Dixon, T. H., Miralles-Wilhelm, F., & Sonenshein, R. (2008). Space-based detection of wetlands' surface water level changes from L-band SAR interferometry. Remote Sensing of Environment, 112(3), 681-696.

Wigneron, J. P., Schmugge, T., Chanzy, A., Calvet, J. C., & Kerr, Y. (1998). Use of passive microwave remote sensing to monitor soil moisture. Agronomie, 18(1), 27-43.

Zhang, B. (2008). Data Mining, GIS and Remote Sensing: Application in wetland hydrological investigation., Ohio State University, Ohio.

VITA

Graduate College
University of Nevada, Las Vegas

Sumit Puri

Degrees:
Bachelor of Engineering, Civil Engineering, 2006.
Punjab Engineering College, Chandigarh, India.

Thesis Title:
Soil Moisture and Water Stage Estimation Using Remote Sensing Techniques.

Thesis Examination Committee:
Committee Chair, Sajjad Ahmad, Ph.D.
Committee Member, Thomas Piechota, Ph.D.
Committee Member, Kumud Acharya, Ph.D.
Graduate Faculty Representative, Ashok Singh. Ph.D.